B. Spire, G. Scarlatti, E. Pesenti, A. G. Siccardi, and A. Beretta. 1999. Enhanced HIV infectivity and changes in GP120 conformation associated with viral incorporation of human leucocyte antigen class I molecules. AIDS **13:**2033–2042.
14. **Cosson, P.** 1996. Direct interaction between the envelope and matrix proteins of HIV-1. EMBO J. **15:**5783–5788.
15. **Dalgleish, A. G., P. C. Beverley, P. R. Clapham, D. H. Crawford, M. F. Greaves, and R. A. Weiss.** 1984. The CD4 (T4) antigen is an essential component of the receptor for the AIDS retrovirus. Nature **312:**763–767.
16. **Davis, M. R., J. Jiang, J. Zhou, E. O. Freed, and C. Aiken.** 2006. A mutation in the human immunodeficiency virus type 1 Gag protein destabilizes the interaction of the envelope protein subunits gp120 and gp41. J. Virol. **80:** 2405–2417.
17. **Deng, H., R. Liu, W. Ellmeier, S. Choe, D. Unutmaz, M. Burkhart, P. Di Marzio, S. Marmon, R. E. Sutton, C. M. Hill, C. B. Davis, S. C. Peiper, T. J. Schall, D. R. Littman, and N. R. Landau.** 1996. Identification of a major co-receptor for primary isolates of HIV-1. Nature **381:**661–666.
18. **Derdeyn, C. A., J. M. Decker, J. N. Sfakianos, X. Wu, W. A. O'Brien, L. Ratner, J. C. Kappes, G. M. Shaw, and E. Hunter.** 2000. Sensitivity of human immunodeficiency virus type 1 to the fusion inhibitor T-20 is modulated by coreceptor specificity defined by the V3 loop of gp120. J. Virol. **74:**8358–8367.
19. **Doranz, B. J., J. Rucker, Y. Yi, R. J. Smyth, M. Samson, S. C. Peiper, M. Parmentier, R. G. Collman, and R. W. Doms.** 1996. A dual-tropic primary HIV-1 isolate that uses fusin and the β-chemokine receptors CKR-5, CKR-3, and CKR-2b as fusion cofactors. Cell **85:**1149–1158.
20. **Dragic, T., V. Litwin, G. P. Allaway, S. R. Martin, Y. Huang, K. A. Nagashima, C. Cayanan, P. J. Maddon, R. A. Koup, J. P. Moore, and W. A. Paxton.** 1996. HIV-1 entry into $CD4^+$ cells is mediated by the chemokine receptor CC-CKR-5. Nature **381:**667–673.
21. **Esser, M. T., D. R. Graham, L. V. Coren, C. M. Trubey, J. W. Bess, Jr., L. O. Arthur, D. E. Ott, and J. D. Lifson.** 2001. Differential incorporation of CD45, CD80 (B7-1), CD86 (B7-2), and major histocompatibility complex class I and II molecules into human immunodeficiency virus type 1 virions and microvesicles: implications for viral pathogenesis and immune regulation. J. Virol. **75:**6173–6182.
22. **Feng, Y., C. C. Broder, P. E. Kennedy, and E. A. Berger.** 1996. HIV-1 entry cofactor: functional cDNA cloning of a seven-transmembrane, G protein-coupled receptor. Science **272:**872–877.
23. **Freed, E. O., and M. A. Martin.** 2001. HIVs and their replication, p. 1971–2041. *In* D. M. Knipe and P. M. Howley (ed.), Fields virology, 4th ed., vol. 2. Lippincott Williams & Wilkins, Philadelphia, PA.
24. **Freed, E. O., and M. A. Martin.** 1995. The role of human immunodeficiency virus type 1 envelope glycoproteins in virus infection. J. Biol. Chem. **270:** 23883–23886.
25. **Giguere, J. F., S. Bounou, J. S. Paquette, J. Madrenas, and M. J. Tremblay.** 2004. Insertion of host-derived costimulatory molecules CD80 (B7.1) and CD86 (B7.2) into human immunodeficiency virus type 1 affects the virus life cycle. J. Virol. **78:**6222–6232.
26. **Gordon-Alonso, M., M. Yanez-Mo, O. Barreiro, S. Alvarez, M. A. Munoz-Fernandez, A. Valenzuela-Fernandez, and F. Sanchez-Madrid.** 2006. Tetraspanins CD9 and CD81 modulate HIV-1-induced membrane fusion. J. Immunol. **177:**5129–5137.
27. **Gould, S. J., A. M. Booth, and J. E. Hildreth.** 2003. The Trojan exosome hypothesis. Proc. Natl. Acad. Sci. USA **100:**10592–10597.
28. **Grigorov, B., F. Arcanger, P. Roingeard, J. L. Darlix, and D. Muriaux.** 2006. Assembly of infectious HIV-1 in human epithelial and T-lymphoblastic cell lines. J. Mol. Biol. **359:**848–862.
29. **Hachiya, A., S. Aizawa-Matsuoka, M. Tanaka, Y. Takahashi, S. Ida, H. Gatanaga, Y. Hirabayashi, A. Kojima, M. Tatsumi, and S. Oka.** 2001. Rapid and simple phenotypic assay for drug susceptibility of human immunodeficiency virus type 1 using CCR5-expressing HeLa/$CD4^+$ cell clone 1–10 (MAGIC-5). Antimicrob. Agents Chemother. **45:**495–501.
30. **Harada, S., Y. Koyanagi, H. Nakashima, N. Kobayashi, and N. Yamamoto.** 1986. Tumor promoter, TPA, enhances replication of HTLV-III/LAV. Virology **154:**249–258.
31. **Harada, S., Y. Koyanagi, and N. Yamamoto.** 1985. Infection of HTLV-III/LAV in HTLV-I-carrying cells MT-2 and MT-4 and application in a plaque assay. Science **229:**563–566.
32. **Hemler, M. E.** 2005. Tetraspanin functions and associated microdomains. Nat. Rev. Mol. Cell Biol. **6:**801–811.
33. **Ho, S. H., F. Martin, A. Higginbottom, L. J. Partridge, V. Parthasarathy, G. W. Moseley, P. Lopez, C. Cheng-Mayer, and P. N. Monk.** 2006. Recombinant extracellular domains of tetraspanin proteins are potent inhibitors of the infection of macrophages by human immunodeficiency virus type 1. J. Virol. **80:**6487–6496.
34. **Janvier, K., and J. S. Bonifacino.** 2005. Role of the endocytic machinery in the sorting of lysosome-associated membrane proteins. Mol. Biol. Cell **16:** 4231–4242.
35. **Jolly, C., and Q. J. Sattentau.** 2007. Human immunodeficiency virus type 1 assembly, budding, and cell-cell spread in T cells take place in tetraspanin-enriched plasma membrane domains. J. Virol. **81:**7873–7884.
36. **Kawano, Y., T. Yoshida, K. Hieda, J. Aoki, H. Miyoshi, and Y. Koyanagi.** 2004. A lentiviral cDNA library employing lambda recombination used to clone an inhibitor of human immunodeficiency virus type 1-induced cell death. J. Virol. **78:**11352–11359.
37. **Klatzmann, D., E. Champagne, S. Chamaret, J. Gruest, D. Guetard, T. Hercend, J. C. Gluckman, and L. Montagnier.** 1984. T-lymphocyte T4 molecule behaves as the receptor for human retrovirus LAV. Nature **312:**767–768.
38. **Kohno, T., Y. Fujioka, T. Goto, S. Morimatsu, C. Morita, T. Nakano, and K. Sano.** 1998. Contrast-enhancement for the image of human immunodeficiency virus from ultrathin section by immunoelectron microscopy. J. Virol. Methods **72:**137–143.
39. **Koyanagi, Y., S. Harada, and N. Yamamoto.** 1986. Establishment of a high production system for AIDS retroviruses with a human T-leukemic cell line Molt-4. Cancer Lett. **30:**299–310.
40. **Koyanagi, Y., S. Miles, R. T. Mitsuyasu, J. E. Merrill, H. V. Vinters, and I. S. Chen.** 1987. Dual infection of the central nervous system by AIDS viruses with distinct cellular tropisms. Science **236:**819–822.
41. **Koyanagi, Y., Y. Tanaka, J. Kira, M. Ito, K. Hioki, N. Misawa, Y. Kawano, K. Yamasaki, R. Tanaka, Y. Suzuki, Y. Ueyama, E. Terada, T. Tanaka, M. Miyasaka, T. Kobayashi, Y. Kumazawa, and N. Yamamoto.** 1997. Primary human immunodeficiency virus type 1 viremia and central nervous system invasion in a novel hu-PBL-immunodeficient mouse strain. J. Virol. **71:**2417–2424.
42. **Lama, J., A. Mangasarian, and D. Trono.** 1999. Cell-surface expression of CD4 reduces HIV-1 infectivity by blocking Env incorporation in a Nef- and Vpu-inhibitable manner. Curr. Biol. **9:**622–631.
43. **Le Naour, F., E. Rubinstein, C. Jasmin, M. Prenant, and C. Boucheix.** 2000. Severely reduced female fertility in CD9-deficient mice. Science **287:**319–321.
44. **Martin, G., Y. Beausejour, J. Thibodeau, and M. J. Tremblay.** 2005. Envelope glycoproteins are dispensable for insertion of host HLA-DR molecules within nascent human immunodeficiency virus type 1 particles. Virology **335:**286–290.
45. **Meerloo, T., H. K. Parmentier, A. D. Osterhaus, J. Goudsmit, and H. J. Schuurman.** 1992. Modulation of cell surface molecules during HIV-1 infection of H9 cells. An immunoelectron microscopic study. AIDS **6:**1105–1116.
46. **Meerloo, T., M. A. Sheikh, A. C. Bloem, A. de Ronde, M. Schutten, C. A. van Els, P. J. Roholl, P. Joling, J. Goudsmit, and H. J. Schuurman.** 1993. Host cell membrane proteins on human immunodeficiency virus type 1 after in vitro infection of H9 cells and blood mononuclear cells. An immuno-electron microscopic study. J. Gen. Virol. **74:**129–135.
47. **Miyado, K., G. Yamada, S. Yamada, H. Hasuwa, Y. Nakamura, F. Ryu, K. Suzuki, K. Kosai, K. Inoue, A. Ogura, M. Okabe, and E. Mekada.** 2000. Requirement of CD9 on the egg plasma membrane for fertilization. Science **287:**321–324.
48. **Murakami, T., and E. O. Freed.** 2000. The long cytoplasmic tail of gp41 is required in a cell type-dependent manner for HIV-1 envelope glycoprotein incorporation into virions. Proc. Natl. Acad. Sci. USA **97:**343–348.
49. **Nguyen, D. H., and J. E. Hildreth.** 2000. Evidence for budding of human immunodeficiency virus type 1 selectively from glycolipid-enriched membrane lipid rafts. J. Virol. **74:**3264–3272.
50. **Nydegger, S., S. Khurana, D. N. Krementsov, M. Foti, and M. Thali.** 2006. Mapping of tetraspanin-enriched microdomains that can function as gateways for HIV-1. J. Cell Biol. **173:**795–807.
51. **Ono, A., S. D. Ablan, S. J. Lockett, K. Nagashima, and E. O. Freed.** 2004. Phosphatidylinositol (4,5) bisphosphate regulates HIV-1 Gag targeting to the plasma membrane. Proc. Natl. Acad. Sci. USA **101:**14889–14894.
52. **Ono, A., and E. O. Freed.** 2004. Cell-type-dependent targeting of human immunodeficiency virus type 1 assembly to the plasma membrane and the multivesicular body. J. Virol. **78:**1552–1563.
53. **Ory, D. S., B. A. Neugeboren, and R. C. Mulligan.** 1996. A stable human-derived packaging cell line for production of high titer retrovirus/vesicular stomatitis virus G pseudotypes. Proc. Natl. Acad. Sci. USA **93:**11400–11406.
54. **Paquette, J. S., J. F. Fortin, L. Blanchard, and M. J. Tremblay.** 1998. Level of ICAM-1 surface expression on virus producer cells influences both the amount of virion-bound host ICAM-1 and human immunodeficiency virus type 1 infectivity. J. Virol. **72:**9329–9336.
55. **Pelchen-Matthews, A., B. Kramer, and M. Marsh.** 2003. Infectious HIV-1 assembles in late endosomes in primary macrophages. J. Cell Biol. **162:**443–455.
56. **Perlman, M., and M. D. Resh.** 2006. Identification of an intracellular trafficking and assembly pathway for HIV-1 Gag. Traffic **7:**731–745.
57. **Planelles, V., F. Bachelerie, J. B. Jowett, A. Haislip, Y. Xie, P. Banooni, T. Masuda, and I. S. Chen.** 1995. Fate of the human immunodeficiency virus type 1 provirus in infected cells: a role for vpr. J. Virol. **69:**5883–5889.
58. **Poignard, P., E. O. Saphire, P. W. Parren, and D. R. Burton.** 2001. gp120: biologic aspects of structural features. Annu. Rev. Immunol. **19:**253–274.
59. **Poon, B., K. Grovit-Ferbas, S. A. Stewart, and I. S. Chen.** 1998. Cell cycle arrest by Vpr in HIV-1 virions and insensitivity to antiretroviral agents. Science **281:**266–269.
60. **Raposo, G., M. Moore, D. Innes, R. Leijendekker, A. Leigh-Brown, P. Bena-**

roch, and H. Geuze. 2002. Human macrophages accumulate HIV-1 particles in MHC II compartments. Traffic **3**:718–729.
61. **Saifuddin, M., C. J. Parker, M. E. Peeples, M. K. Gorny, S. Zolla-Pazner, M. Ghassemi, I. A. Rooney, J. P. Atkinson, and G. T. Spear.** 1995. Role of virion-associated glycosylphosphatidylinositol-linked proteins CD55 and CD59 in complement resistance of cell line-derived and primary isolates of HIV-1. J. Exp. Med. **182**:501–509.
62. **Stipp, C. S., T. V. Kolesnikova, and M. E. Hemler.** 2003. Functional domains in tetraspanin proteins. Trends Biochem. Sci. **28**:106–112.
63. **Suzuki, Y., Y. Koyanagi, Y. Tanaka, T. Murakami, N. Misawa, N. Maeda, T. Kimura, H. Shida, J. A. Hoxie, W. A. O'Brien, and N. Yamamoto.** 1999. Determinant in human immunodeficiency virus type 1 for efficient replication under cytokine-induced CD4$^+$ T-helper 1 (Th1)- and Th2-type conditions. J. Virol. **73**:316–324.
64. **Suzuki, Y., N. Misawa, C. Sato, H. Ebina, T. Masuda, N. Yamamoto, and Y. Koyanagi.** 2003. Quantitative analysis of human immunodeficiency virus type 1 DNA dynamics by real-time PCR: integration efficiency in stimulated and unstimulated peripheral blood mononuclear cells. Virus Genes **27**:177–188.
65. **Takeda, Y., I. Tachibana, K. Miyado, M. Kobayashi, T. Miyazaki, T. Funakoshi, H. Kimura, H. Yamane, Y. Saito, H. Goto, T. Yoneda, M. Yoshida, T. Kumagai, T. Osaki, S. Hayashi, I. Kawase, and E. Mekada.** 2003. Tetraspanins CD9 and CD81 function to prevent the fusion of mononuclear phagocytes. J. Cell Biol. **161**:945–956.
66. **Tanaka, M., T. Ueno, T. Nakahara, K. Sasaki, A. Ishimoto, and H. Sakai.** 2003. Downregulation of CD4 is required for maintenance of viral infectivity of HIV-1. Virology **311**:316–325.
67. **Tardif, M. R., and M. J. Tremblay.** 2003. Presence of host ICAM-1 in human immunodeficiency virus type 1 virions increases productive infection of CD4$^+$ T lymphocytes by favoring cytosolic delivery of viral material. J. Virol. **77**:12299–12309.
68. **Tarrant, J. M., L. Robb, A. B. van Spriel, and M. D. Wright.** 2003. Tetraspanins: molecular organisers of the leukocyte surface. Trends Immunol. **24**:610–617.
69. **Trubey, C. M., E. Chertova, L. V. Coren, J. M. Hilburn, C. V. Hixson, K. Nagashima, J. D. Lifson, and D. E. Ott.** 2003. Quantitation of HLA class II protein incorporated into human immunodeficiency type 1 virions purified by anti-CD45 immunoaffinity depletion of microvesicles. J. Virol. **77**:12699–12709.
70. **von Lindern, J. J., D. Rojo, K. Grovit-Ferbas, C. Yeramian, C. Deng, G. Herbein, M. R. Ferguson, T. C. Pappas, J. M. Decker, A. Singh, R. G. Collman, and W. A. O'Brien.** 2003. Potential role for CD63 in CCR5-mediated human immunodeficiency virus type 1 infection of macrophages. J. Virol. **77**:3624–3633.
71. **Wright, M. D., J. Ni, and G. B. Rudy.** 2000. The L6 membrane proteins—a new four-transmembrane superfamily. Protein Sci. **9**:1594–1600.
72. **Wyma, D. J., J. Jiang, J. Shi, J. Zhou, J. E. Lineberger, M. D. Miller, and C. Aiken.** 2004. Coupling of human immunodeficiency virus type 1 fusion to virion maturation: a novel role of the gp41 cytoplasmic tail. J. Virol. **78**: 3429–3435.
73. **Wyma, D. J., A. Kotov, and C. Aiken.** 2000. Evidence for a stable interaction of gp41 with Pr55^{Gag} in immature human immunodeficiency virus type 1 particles. J. Virol. **74**:9381–9387.
74. **Zagury, D., J. Bernard, R. Leonard, R. Cheynier, M. Feldman, P. S. Sarin, and R. C. Gallo.** 1986. Long-term cultures of HTLV-III-infected T cells: a model of cytopathology of T-cell depletion in AIDS. Science **231**:850–853.

Traffic 2008; 9: 540–558
Blackwell Munksgaard

doi: 10.1111/j.1600-0854.2007.00700.x

A CD63 Mutant Inhibits T-cell Tropic Human Immunodeficiency Virus Type 1 Entry by Disrupting CXCR4 Trafficking to the Plasma Membrane

Takeshi Yoshida[1], Yuji Kawano[2], Kei Sato[1], Yoshinori Ando[1], Jun Aoki[1], Yoshiharu Miura[1], Jun Komano[3], Yuetsu Tanaka[4] and Yoshio Koyanagi[1,*]

[1]Laboratory of Viral Pathogenesis, Institute for Virus Research, Kyoto University, Sakyo-ku, Kyoto 606-8507, Japan
[2]Department of Neurology, Neurological Institute, Graduate School of Medical Science, Kyushu University, Higashi-ku, Fukuoka 812-8582, Japan
[3]AIDS Research Center, National Institute of Infectious Diseases, Shinjuku-ku, Tokyo 162-8640, Japan
[4]Department of Immunology, Graduate School of Medicine, University of the Ryukyus, Nishihara, Okinawa 903-0215, Japan
**Corresponding author: Yoshio Koyanagi, ykoyanag@virus.kyoto-u.ac.jp*

We have discovered that an N-terminal deletion mutant of a membrane protein, CD63, (CD63ΔN) blocks entry of CXCR4-using, T-cell tropic human immunodeficiency virus type 1 (X4 HIV-1) by suppressing CXCR4 surface expression. This suppression was observed for CXCR4 but not for CD4, CCR5, CD25, CD71 or other tetraspanin proteins. The suppression of CXCR4 expression on the plasma membrane appeared to be caused by mislocalization of CXCR4 and exclusive transportation of CXCR4 toward intracellular organelles, mainly late endosomes/lysosomes. Our data suggest that CXCR4 trafficking can be modified in terms of its recruitment to the plasma membrane without enhancing the degradation or arresting vesicular transport of CXCR4.

Key words: cell surface expression, CD63, CXCR4, HIV-1, ligand-independent trafficking

Received 30 November 2007, revised and accepted for publication 27 December 2007, uncorrected manuscript published online 30 December 2007, published online 13 February 2008

It has been formerly shown that some cellular factors have the ability to suppress retroviral replication. Restriction factors, such as APOBEC3G and Trim5α, play a significant role in controlling human immunodeficiency virus type 1 (HIV-1) infection (1), and it is predicted that other cellular factors will also influence HIV-1 replication. Innovative approaches should, therefore, bring to light, as-yet untested, antiviral factors. We have previously reported a cDNA-library-expressing lentiviral vector system used to isolate an inhibitor of HIV-1-induced cytopathic effect (CPE) (2).

HIV-1 infects T cells and macrophages that express surface CD4 and chemokine receptors. CXCR4 is a G-protein-coupled chemokine receptor that acts as a receptor for stromal-cell-derived factor 1 (SDF-1) and one of the co-receptors for HIV-1 (3). SDF-1 has been shown to inhibit X4 HIV-1 infection, probably by promoting removal of CXCR4 from the cell surface via ligand-induced endocytosis (4,5). The endocytosis of CXCR4 from the cell surface occurs through clathrin-coated pits, which results from the binding to β-arrestin and perhaps adaptor protein complex-2 (AP-2) (5–7). The ubiquitination of CXCR4 at the plasma membrane has been shown to facilitate a sorting event leading to its lysosome-dependent degradation (8,9). In general, membrane proteins are synthesized in the endoplasmic reticulum (ER) and the folded proteins are transported through the Golgi apparatus, and undergo modification such as glycosylation. At the *trans*-Golgi network (TGN), mature proteins are subsequently sorted and packaged into specific vesicles destined for the plasma membrane or the endosomes. In the case of lysosome-associated proteins (LAMP), there are two alternative routes from the TGN, one to the plasma membrane and the other to the lysosomes (10). However, it is unclear whether or not CXCR4 can be targeted directly from the TGN to the lysosome. In addition, there has not been a report of any molecule that affects trafficking of CXCR4 to the plasma membrane.

CD63 is a membrane protein belonging to the tetraspanin superfamily, consisting of four transmembrane domains (TM1-4) and two extracellular (EC) domains (1–2). It is widely expressed on the surface of many cell types, forming tetraspanin-enriched microdomains (TEMs) on the plasma membrane with other tetraspanin proteins (11). It is also present in secretory vesicles (12,13) and the membranes of the late endosomes and lysosomes (14,15). At the plasma membrane, CD63 is known to interact with molecules such as integrins (16), a tissue inhibitor of metalloproteinase-1 (17) and syntenin-1 (18), and is thought to regulate signal transduction pathways required for cell adhesion, motility and survival. It was also reported that CD63 is involved with endocytosis of its interaction partners such as the β-subunit of H, K-ATPase (HKβ) (19) or membrane-type 1 matrix metalloproteinase (MT1-MMP) (20). However, its physiological role is still not well understood (21–23).

In this study, by using our screening strategy (2), we identified an N-terminal deletion mutant of CD63 that

belongs to a novel class of HIV-1 entry blockers. This CD63 mutant appeared to suppress CXCR4 on the cell surface by changing CXCR4 intracellular trafficking probably after its dispatch from the TGN. In addition, we found that wild-type CD63 also functions to suppress CXCR4 cell surface expression, which may be a physiological function of the protein.

Results

Isolation of gene encoding an anti-HIV-1 protein

Using a bicistronic lentiviral vector, encoding cDNA and a humanized recombinant green fluorescent protein (hrGFP), we generated a human peripheral blood leukocyte (PBL) cDNA library-transduced $CD4^+$ $CXCR4^+$ T-cell line (MT-4) (2). Although most cells were killed after X4 HIV-1 (HIV-1_{NL4-3}) infection, some $hrGFP^+$ ($cDNA^+$) cells were found to proliferate continuously for more than 30 days post-infection (dpi), from which it was inferred that these cells were transduced with an anti-HIV-1 cDNA. From these cells, we independently isolated two cDNA clones, each containing a 3′ fragment of *cd63* cDNA spanning nucleotide positions 193 or 228 to the 3′ poly-A sequence (Figure S1). These cDNAs (designated clone 12.03 and clone 12.22, respectively) encode a C-terminal fragment of CD63 that contains 156 amino acid residues (amino acid positions 83–238) initiating from the third methionine (Figure S1). We then confirmed that both clone 12.03 cDNA- and clone 12.22 cDNA-transduced MT-4 cells ($hrGFP^+$) were resistant against HIV-induced CPE (data not shown) and found that there is little expression of HIV-1 antigen on these cells after HIV-1 inoculation (Figure 1A). Thus, we isolated cDNAs as a new inhibitor gene of HIV-1-induced CPE.

To reproduce this inhibition via transduction of the *cd63* gene, we next prepared a wild-type *cd63* cDNA (CD63wt)-expressing lentiviral vector, as well as an N-terminal deletion mutant (CD63ΔN)-expressing lentiviral vector (Figure 1B) encoding a C-terminal fragment of CD63 identical to those of the isolated cDNA clones mentioned above (Figure S1). Western blotting analysis using an anti-CD63 monoclonal antibody (mAb), confirmed that CD63ΔN-expressing lentiviral vector and the two originally-isolated cDNA expressed peptides with identical molecular weight (MW) (data not shown). As CD63 has a tyrosine-based lysosomal sorting motif (LSM; amino acid positions 233–238) that binds to AP-2 μ and AP-3 μ subunits (15), we also prepared an LSM-deleted CD63ΔN mutant (designated CD63ΔNL) (Figure 1B). FLAG-tagged wild-type CD63 (FLAGCD63wt), CD63ΔN (FLAGCD63ΔN), or CD63ΔNL (FLAGCD63ΔNL) DNA was transfected into HeLa-derived MAGIC-5 cells ($CXCR4^+$ $CD4^+$ $CCR5^+$), and expression was confirmed by Western blotting using an anti-FLAG mAb. This revealed that these proteins were heavily glycosylated (Figure 1C). Immunofluorescent analysis using these DNA showed that CD63wt and CD63ΔN was predominantly distributed in the perinuclear region and some CD63ΔN were found in intracellular vesicles (Figure 1D). The majority of CD63ΔNL, however, appeared to accumulate at the plasma membrane with some intracellular staining (Figure 1D, third panel).

Inhibition of HIV-1 infection by transduction of cells with CD63 and CD63 mutants

To examine anti-HIV-1 activity of CD63-transduced cells further, we generated ectopic CD63wt- or CD63 mutant-expressing cells using a bicistronic $H2K^k$-expressing lentiviral vector. Transduction of the gene by this lentiviral vector did not substantially affect cell growth (data not shown). We then evaluated anti-HIV activity using an enhanced GFP (EGFP)-expressing X4 HIV-1 (NL-EGFP) (24). Flow cytometric analyses indicated that HIV-1 infection was clearly inhibited in the CD63wt- and CD63 mutant (i.e. CD63ΔN and CD63ΔNL)-transduced cells compared with untransduced or empty vector-transduced cells. In CD63ΔN-transduced cells, in particular, HIV-1 infection was severely inhibited (Figure 1E, fourth panel). However, when we used a pseudotyped HIV-1 (where the HIV-1 envelope protein was replaced with that of amphotropic Moloney murine leukemia virus, MLV), the infectivity reduction was not observed (Figure 1F), suggesting that this inhibition is virus envelope protein dependent.

We confirmed that CD63ΔN was also able to protect transduced cells against wild-type X4 HIV-1 infection. Following X4 HIV-1_{NL4-3} infection, enzyme-linked immunosorbent assays (ELISA) revealed that the level of HIV-1 $p24^{gag}$ protein in the culture supernatant of CD63ΔN-transduced MT-4 and MAGIC-5 cells was approximately 100-fold lower than that of either empty vector-transduced or untransduced cells (Figure 1G, left and center panels). However, in the case of CCR5-using HIV-1 (R5 HIV-1; HIV-1_{JR-CSF}) infection, there was no apparent effect of CD63ΔN on the concentration of $p24^{gag}$ in the culture supernatant (Figure 1G, right panel). These data suggest that replication of X4 HIV-1 was specifically inhibited by CD63ΔN. In addition, the level of newly synthesized X4 HIV-1 cDNA in the CD63ΔN-transduced cells was clearly lower (Figure 1H), suggesting that entry of X4 HIV-1 was inhibited by CD63ΔN. Taken together, these results suggest that ectopic CD63wt and CD63ΔN specifically inhibit X4 HIV-1 entry. Therefore, we hypothesized that expression of the X4 virus-specific co-receptor molecule, CXCR4, might be downregulated by ectopic expression of CD63wt and CD63ΔN.

Suppression of CXCR4 surface expression by CD63- and its mutant transduction

To examine the correlation between levels of CXCR4 surface expression and the transduction efficiency of CD63wt and its mutants, we transduced CD63 into cells in different multiplicity of infection (MOI) using a bicistronic $H2K^k$-expressing lentiviral vector. Flow cytometric analysis using an anti-$H2K^k$ mAb confirmed that higher MOI increased transduction efficiency (data not shown). The flow cytometric analyses using an anti-CXCR4 mAb (A-80)

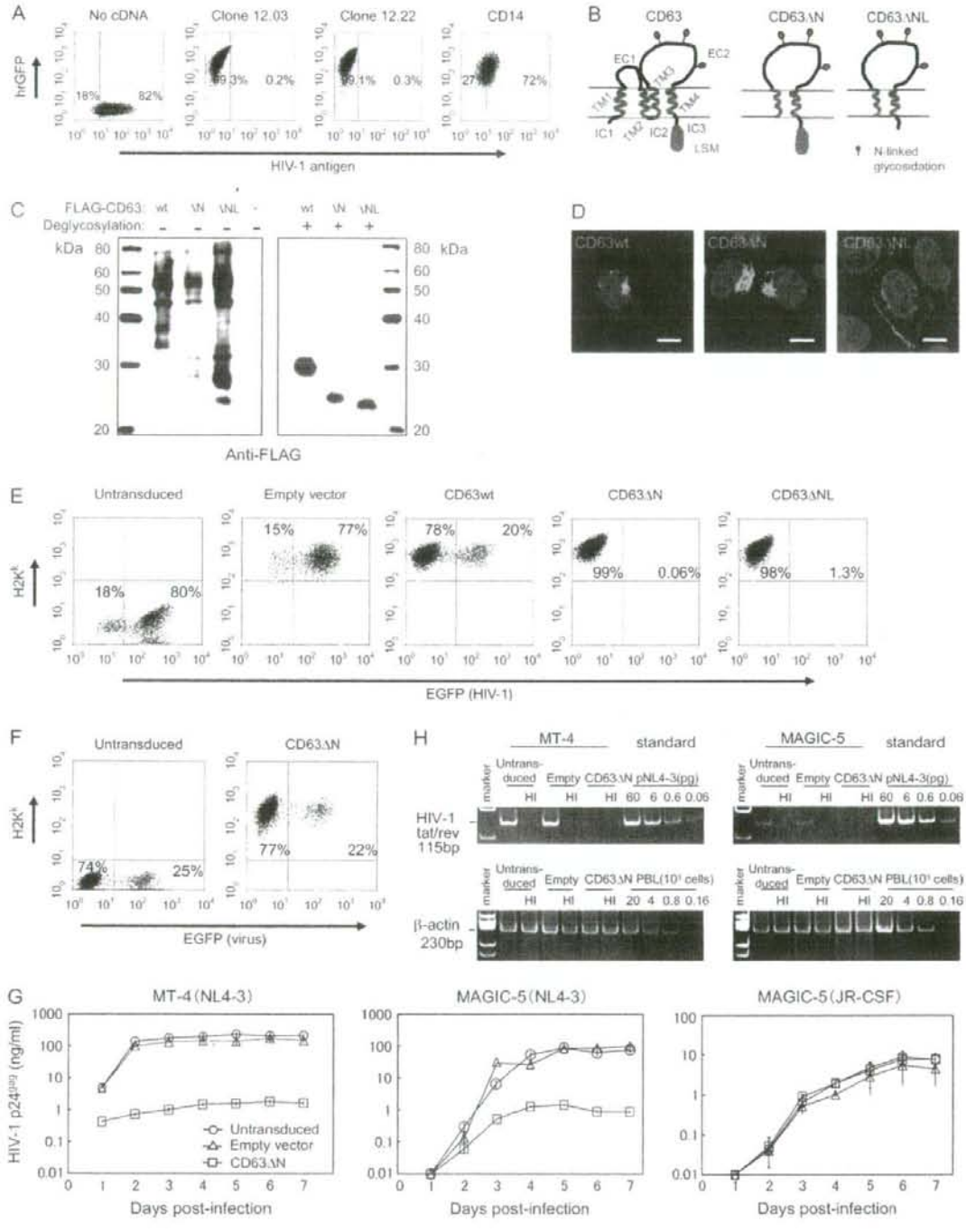

Figure 1: Legend on next page.

indicated that the level of CXCR4 surface expression on CD63wt-transduced MT-4 cells clearly decreased with increased MOI (Figure 2A). A much more obvious suppression of CXCR4 surface expression was found on CD63ΔN-transduced cells (Figure 2A). The suppression of CXCR4 surface expression was further confirmed using another anti-CXCR4 mAb (12G5) (25), which reacts with a different epitope (data not shown). The CD63ΔN-induced suppression of CXCR4 surface expression was only partially impaired by LSM deletion (CD63ΔNL in Figure 2A), and a CD63 mutant lacking LSM (CD63ΔL) still has suppressive activity (data not shown). Suppression of cell surface expression of CXCR4 was also found in 293T cells co-transfected with CXCR4 and CD63ΔN DNA (data not shown).

Suppression of surface expression in CD63wt or CD63 mutant-transduced MT-4 cells was detectable only in CXCR4, but not in CD25 [interleukin (IL)-2 receptor α chain] (Figure 2B), or CD71 (transferrin receptor) molecules (Figure 2C). The suppression of CXCR4, but not CCR5, CD4 or CD71 was also found in CD63ΔN-transduced MAGIC-5 cells (Figure 2D). In addition, the suppression of other tetraspanin proteins such as CD9, CD53, CD81, CD82 and CD151 was not found in CD63ΔN-transduced MAGIC-5 cells (data not shown). Fluorescent microscopic analysis on live cells, using a third anti-CXCR4 mAb (A-145), confirmed the loss of surface CXCR4 on CD63ΔN-transduced MAGIC-5 cells (Figure 2E). Significant suppression was also seen in human $CD4^+$ T cells derived from peripheral blood mononuclear cells (PBMC), which are natural target cells for HIV-1 (Figure 2F). To further confirm the CXCR4 suppression, we assessed the ability of the transduced cells to migrate in response to SDF-1 stimulation. We treated CD63ΔN-transduced MAGIC-5 cells with SDF-1 and found a severe suppression of chemotaxis response in CD63ΔN-transduced cells compared with that of empty vector-transduced cells (Figure 2G). From these results, we concluded that ectopic CD63, especially CD63ΔN, induces significant downregulation of CXCR4 surface expression, because it (i) protects cells against X4 HIV-1 infection, (ii) renders cell surface expression of CXCR4 undetectable when analyzed using 3 anti-CXCR4 mAbs or (iii) renders cells unable to respond to SDF-1.

Involvement of CD63 in regulation of CXCR4 cell surface expression

To clarify whether physiological CD63 plays a role in the regulation of CXCR4 surface expression, we next depleted endogenous CD63 in empty vector-transduced cells using three small interfering RNA (siRNA) oligonucleotides against *cd63*. Immunofluorescent analysis indicated a clear depletion of intracellular CD63 by these siRNAs compared with control siRNA (Figure 3A). Flow cytometric analysis also indicated a significant reduction in CD63 surface expression by these siRNAs (Figure 3B). Levels of CXCR4 surface expression on *cd63*-depleted cells were clearly higher than that on control cells (Figure 3C), indicating that depletion of CD63 resulted in an increased level of CXCR4 surface expression. Combined with the data from CD63wt-transduced cells (Figure 2A), we deduced that CD63 may also negatively regulate CXCR4 surface expression.

Induction of CXCR4 mislocalization by CD63ΔN

To address how CD63ΔN suppresses CXCR4 surface expression, we considered the following possibilities: (i) suppression of CXCR4 mRNA or protein expression;

Figure 1: Specific inhibition of X4 HIV-1 infection by CD63 mutants. A) Little expression of HIV-1 antigen was detected in MT-4 cells transduced with the two putative CD63 C-terminal cDNAs (clone 12.03 and clone 12.22). Four days after HIV-1_{NL4-3} infection, HIV-1 antigen expression on transduced cells was examined using anti-HIV-1 human sera. The level of hrGFP indicates the efficiency of cDNA transduction (y-axis). The numbers in each quadrant indicate the percentage of HIV antigen (+) and (−) cells. CD14 is a control having some level of anti-HIV-1 activity as we have previously reported (2). The results of one of three, independently conducted, experiments are shown. B) Structure of CD63 and its mutants. CD63 is comprised of four transmembrane domains (TMs), a small extracellular loop (EC1), a four amino acid intracellular loop (IC2), and a large extracellular loop (EC2), as well as 11 amino acid N-terminal and a 10 amino acids C-terminal tail (containing the LSM). C) CD63 and its mutants are heavily glycosylated. MAGIC-5 cells were transfected with FLAGCD63wt or FLAGCD63-mutant DNA. Cell extracts were incubated in the presence (right panel) or absence (left panel) of deglycosidase and then subjected to Western blot analysis using an anti-FLAG mAb. D) Localization of CD63wt and CD63 mutants. MAGIC-5 cells were transfected with FLAGCD63wt or FLAGCD63-mutant DNA, stained with an anti-FLAG mAb, and analyzed by confocal microscopy. Images were acquired through band-pass filters (BPF) 500–520 nm (FLAG: green) and BPF 420–470 nm (Hoechst; nuclei staining: blue). Scale bars, 10 μm. E) Inhibition of HIV-1 infection by transduction of CD63wt or CD63 mutants. CD63wt-, CD63ΔN-, and CD63ΔNL-transduced MT-4 cells were challenged with NL-EGFP at a MOI of 0.1. Three days after HIV-1 infection, cells were stained with an anti-$H2K^k$mAb, and analyzed by flow cytometry. Surface expression of $H2K^k$gave an indication of transduction efficiency (y-axis). The numbers in each quadrant indicate the percentage of EGFP (+) and (−) cells. The results of one of three, independently conducted, experiments are shown. F) No inhibition of MLV Env-pseudotyped HIV-1 infection by transduction of CD63ΔN. CD63ΔN-transduced MT-4 cells were also challenged with an amphotropic MLV Env-pseudotyped EGFP-expressing HIV-1. The numbers in each quadrant indicate the percentage of EGFP (+) and (−) cells. The results of one of three, independently conducted, experiments are shown. G) Lower X4 HIV-1 production in CD63ΔN-transduced cells. The amount of HIV $p24^{gag}$ in cell culture supernatant was followed using ELISA after wild-type HIV-1 infection (left panel: X4 HIV-1_{NL4-3}-infected MT-4 cells; center panel: X4 HIV-1_{NL4-3}-infected MAGIC-5 cells; and right panel: R5 HIV-1_{JR-CSF}-infected MAGIC-5 cells). H) Blocking of X4 HIV-1 entry in CD63ΔN-transduced cells. The level of synthesized HIV-1 cDNA in cells was semiquantified by PCR. HI indicates heat inactivated HIV-1. HIV-1 plasmid DNA was used for marker standards (left: X4 HIV-1_{NL4-3}-infected MT-4 cells; and right: X4 HIV-1_{NL4-3}-infected MAGIC-5 cells). β-actin serves as a control.

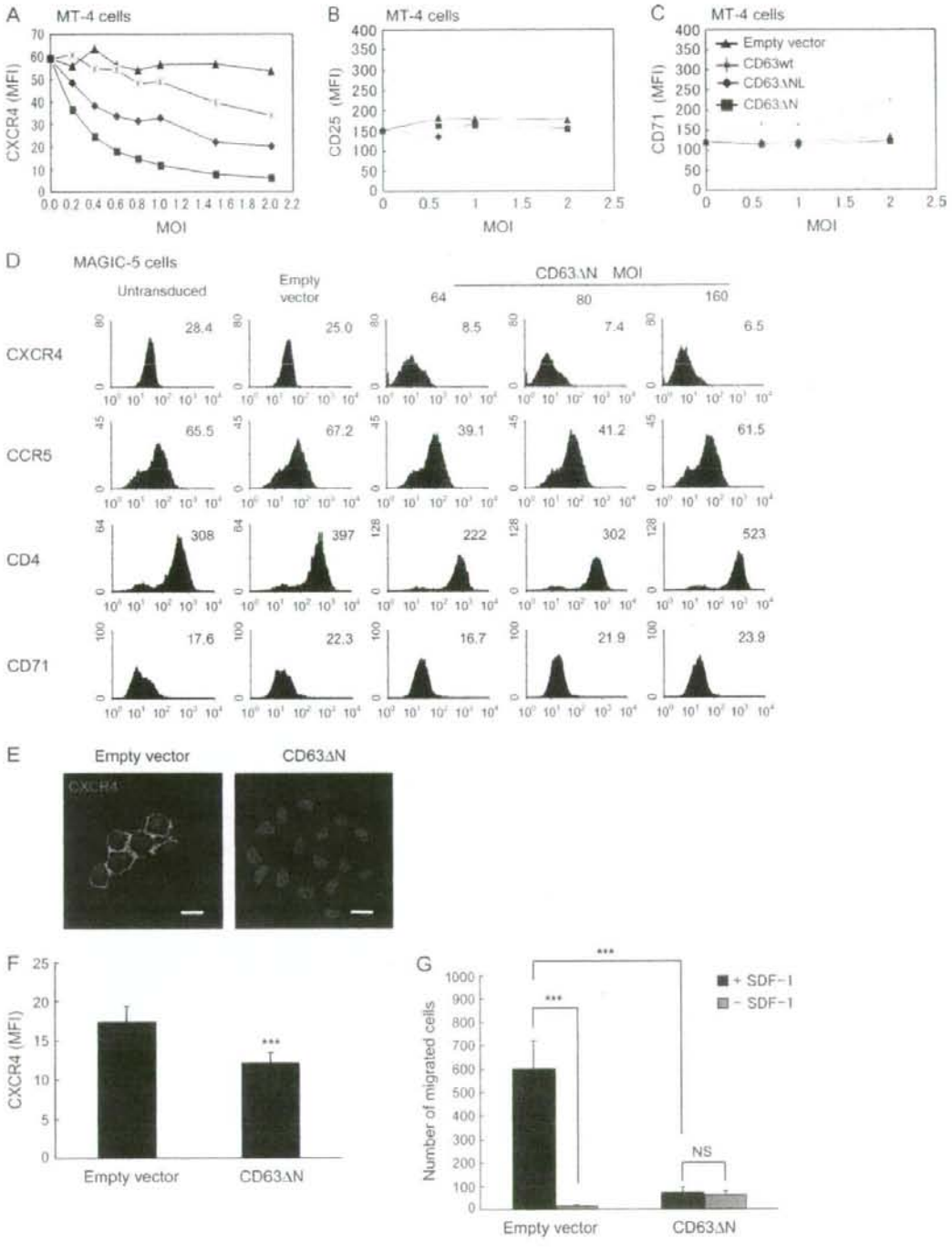

Figure 2: Legend on next page.

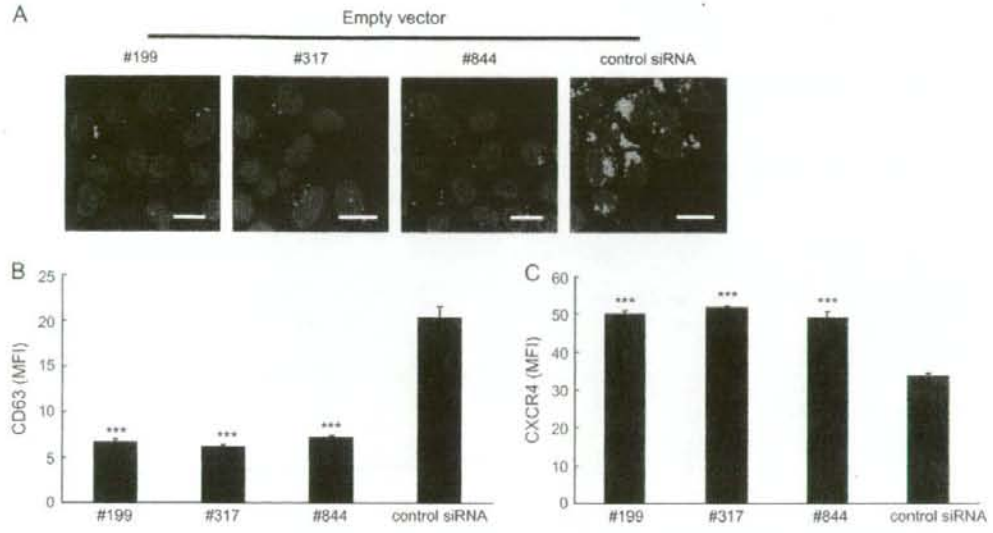

Figure 3: Suppression of CXCR4 surface expression by endogenous CD63. (A) Efficient depletion of endogenous CD63. Empty vector-transduced MAGIC-5 cells were transfected with siRNA oligonucleotides against *cd63* or control siRNA, then stained with an anti-CD63 mAb, and analyzed by confocal microscopy. Images were acquired through band-pass filters (BPF) 500–520 nm (CD63: green) and BPF 420-470 nm (Hoechst: blue). Scale bar, 30 μm. (B, C) Significant reduction of CD63 and augmentation of CXCR4 surface expression on *cd63*-depleted MAGIC-5 cells. CD63 (B) or CXCR4 (C) expression on empty vector-transduced cells treated with siRNA oligonucleotides against *cd63* was measured by flow cytometry. Data are represented as mean ± SED, $n = 3$, $^{***}P < 0.05$ (vs. control siRNA).

(ii) disappearance of CXCR4 protein because of its rapid degradation; or (iii) mislocalization of CXCR4 protein.

Firstly, we compared the amounts of CXCR4 protein in untransduced cells and cells transduced with CD63ΔN or empty vector. Western blotting analysis indicated that the total amounts of CXCR4 protein were very similar in these cells (Figure 4A), suggesting that possibility (i) can be eliminated.

Next, we compared the rate of CXCR4 degradation in empty vector- and CD63ΔN-transduced cells. From examination of CXCR4 expression in cells transfected with pHA-CXCR4 after cycloheximide (CHX) treatment, an inhibitor of translation, we found that the degradation rate of CXCR4 was very similar between empty vector- and CD63ΔN-transduced MAGIC-5 cells (Figure 4B). Under the same condition, we found that little CD63ΔN degradation occurred (data not shown). These data suggest that possibility (ii) can be eliminated.

From immunofluorescent staining, we found that there was a large amount of intracellular CXCR4 in CD63ΔN-transduced cells, while the majority of CXCR4 localized at the plasma membrane in untransduced or empty vector-transduced cells (Figure 4C). To confirm this phenomenon, we next transfected an hrGFP-tagged CXCR4 DNA (phrGFPCXCR4) into empty vector- or CD63ΔN-transduced MAGIC-5 cells. This enabled us to visualize the location of CXCR4 molecules in live cells. CXCR4 was predominantly

Figure 2: Suppression of CXCR4 surface expression by CD63 or CD63 mutants. A–C) The surface expression of CXCR4 (A), CD25 (B) or CD71 (C) on CD63wt- or CD63 mutant-transduced MT-4 cells was measured by flow cytometry. The *x*-axis indicates MOI of lentiviral vector and *y*-axis indicates the mean fluorescence intensity (MFI). A-80 mAb was used for CXCR4-staining. D) Surface expression of CXCR4, CCR5, CD4 or CD71 on CD63ΔN-transduced MAGIC-5 cells was measured by flow cytometry. The number in each panel indicates the MFI of each molecule. E) The disappearance of CXCR4 on the cell surface of CD63ΔN-transduced MAGIC-5 cells. Empty vector- or CD63ΔN-transduced cells were incubated with another anti-CXCR4 mAb (A-145) at 4°C without permeabilization and analyzed by confocal microscopy. Images were acquired through band-pass filters (BPF) 500–520 nm (CXCR4: green) and BPF 420–470 nm (Hoechst: blue). Scale bars, 20 μm. F) Surface expression of CXCR4 on the CD63ΔN-transduced human $CD4^+$ T cells derived from PBMC. Six days after transduction, cells were stained with an anti-CXCR4 mAb (A-80) and analyzed. MFI of CXCR4 is shown. Data are represented as mean ± SED, $n = 4$, $^{***}P < 0.05$ (vs. empty vector). G) Chemotactic response of MAGIC-5 cells to SDF-1 was reduced by transduction of CD63ΔN. Cells were cultured in the presence (black filled) or absence (grey filled) of SDF-1. Chemokine-mediated migration of cells is expressed as the mean number of migrated cells per three examined fields. Data are represented as mean ± SED, $n = 3$, $^{***}P < 0.05$, NS, not significant.

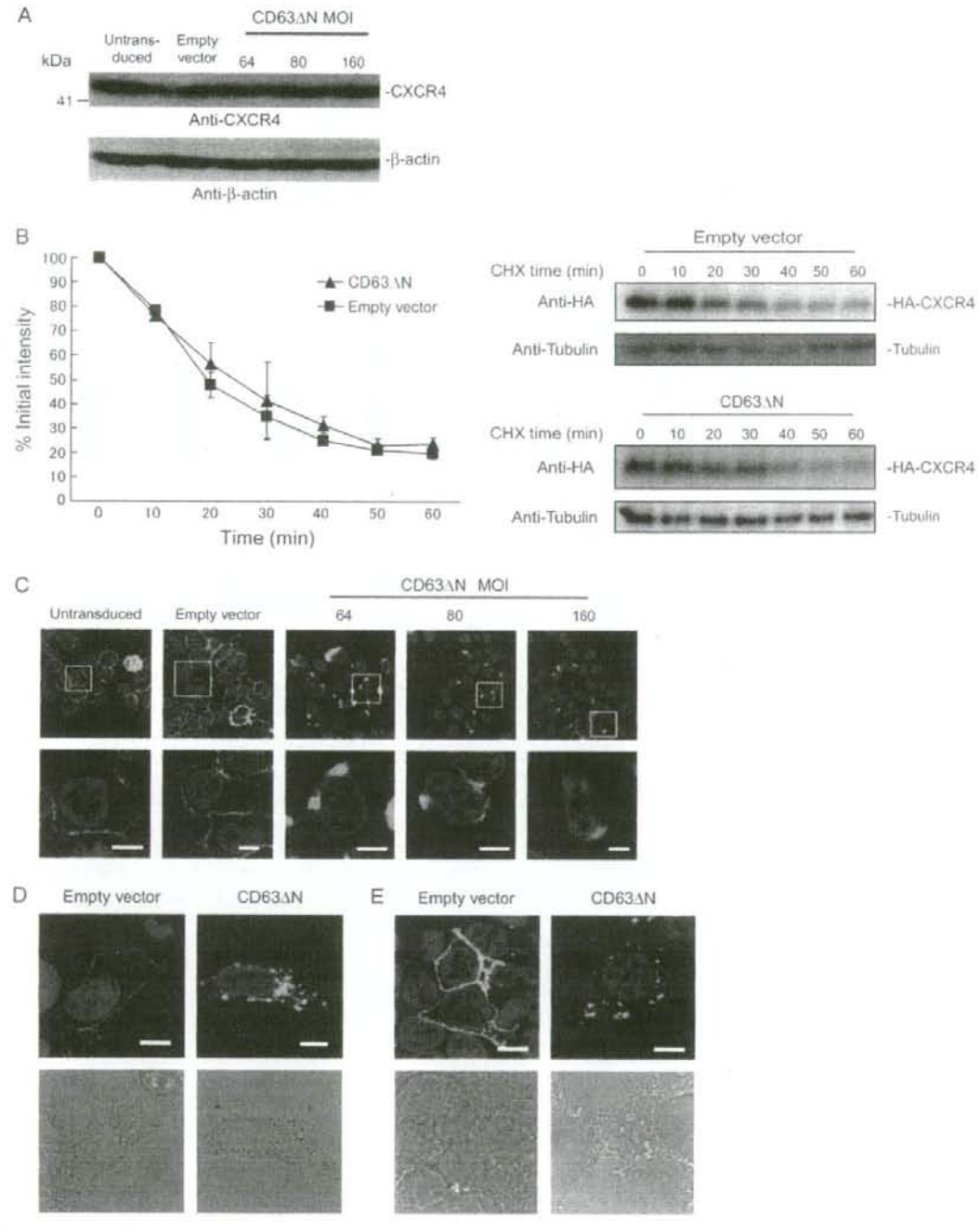

Figure 4: Legend on next page.

localized at the plasma membrane in empty vector-transduced cells, while large amounts of intracellular CXCR4 was found in CD63ΔN-transduced cells (Figure 4D). Intracellular CXCR4 was also found in 293T cells co-transfected with CD63ΔN DNA and phrGFPCXCR4 (Figure 4E). These data strongly suggest that CD63ΔN induces the mislocalization of CXCR4, in which localization of CXCR4 was shifted from the plasma membrane to intracellular membrane.

The mislocalization of CXCR4 might not be due to dynamin-dependent internalization

To clarify the mechanism of this mislocalization, we hypothesized that in CD63ΔN-transduced cells, (i) endocytosis of CXCR4 from the cell surface is strongly augmented; (ii) the intracellular trafficking of CXCR4 via vesicular transport is inhibited or (iii) CXCR4 is transported only to intracellular organelles. To examine CXCR4 surface expression on live cells over a set period of time, we cultured empty vector- or CD63ΔN-transduced MAGIC-5 cells in the presence of an fluorescein isothiocyanate (FITC)-conjugated anti-CXCR4 mAb and then assessed CXCR4 surface expression using confocal microscopy (Figure 5A). Thirty minutes after initiation of culture, CXCR4 was detected on the plasma membrane of empty vector-transduced cells (Figure 5A,c) but not visible on CD63ΔN-transduced cells (Figure 5A,e). Small green spots, probably unspecifically endocytosed or pinocytosed mAb, were also detected not only in cells cultured with anti-CXCR4 mAbs (Figure 5A,c.e) but also in cells cultured with an FITC-conjugated control immunoglobulin (Ig) G (Figure 5A,a). We next carried out the similar experiment in the presence of an actin polymerization inhibitor, cytochalasin D, and confirmed that there was little captured control IgG (Figure 5A,g). In this condition, CXCR4 on the plasma membrane was detected only in empty vector-transduced cells (Figure 5A,i), but not visible in CD63ΔN-transduced cells (Figure 5A,k). CXCR4 on the cell surface was not detected in CD63ΔN-transduced cells after further incubation (120 min) (Figure 5A,o). In addition, we transfected a dominant negative mutant of dynamin 1 (Dynamin 1 K44A) DNA into CD63ΔN-transduced MAGIC-5 cells to block dynamin-dependent CXCR4 internalization (7,8). Although we found the accumulation of transferrin receptor (CD71) on the cells after transfection with Dynamin 1 K44A DNA, we could not observe any recovery of CXCR4 surface expression in the cells (Figure 5B). These data suggest that the CD63ΔN-induced CXCR4 mislocalization might not be the result of dynamin-dependent internalization.

Intracellular trafficking of CXCR4 via transport vesicles is not inhibited in CD63Δ N-transduced cells

To examine the longitudinal distribution of CXCR4 molecules in live cells, we prepared a haloalkane dehalogenase-tagged (Halo-tagged) CXCR4 DNA (pHalo-CXCR4) and transfected it into empty vector- or CD63ΔN-transduced MAGIC-5 cells. After staining with HaloTag™-specific labeling ligand (Halo-ligand), we found that CXCR4 was localized predominantly at the plasma membrane and partly in the intracellular compartment including ceramide$^+$ Golgi apparatus of empty vector-transduced cells (Figure 6A, upper left panel). The labeled CXCR4 at the plasma membrane was rapidly internalized after SDF-1 stimulation (data not shown), indicating that Halo-tagged CXCR4 represents natural CXCR4 distribution. In CD63ΔN-transduced cells, however, we detected most CXCR4 in the intracellular membrane containing the ceramide$^+$ Golgi apparatus, but not at the plasma membrane (Figure 6A, upper center panel). In addition, we observed many vesicle-like CXCR4$^+$ ceramide$^-$ spots in the cytoplasm of these cells (arrow heads in Figure 6A upper center panel). To confirm rigidly that the signal of these spots reflected the existence of Halo-tagged CXCR4, we treated transfected cells with Brefeldin A (BFA), an inhibitor of vesicle transport from the ER to the Golgi apparatus. We detected only reticulated distribution of CXCR4 but no vesicle-like spots in the treated cells (Figure 6A, right panel), confirming that these spots were CXCR4-containing vesicles. The longitudinal distribution of CXCR4 was next traced over 30-min time intervals (Figure 6B,C). Although we detected many CXCR4-containing vesicles during observation (arrow heads in Figure 6C), no CXCR4 at the plasma membrane was found in CD63ΔN-transduced cells. To further examine CXCR4-containing vesicles in detail, we performed analyses using total internal reflection fluorescence microscopy (TIRFM). This microscopy is adequate to trace vesicles within approximately 150 nm of the plasma membrane (adhered surface). We transfected CXCR4EGFP into empty vector- or CD63ΔN-transduced MAGIC-5 cells and successfully detected many CXCR4-containing vesicles (Figure 6D,E, upper left panels). We found a similar

Figure 4: Induction of CXCR4 mislocalization by CD63ΔN. A) Total CXCR4 expression is similar independent of CD63ΔN-transduction in MAGIC-5 cells. The total amounts of CXCR4 protein in empty vector- or CD63ΔN-transduced cells was measured by Western blotting using an anti-CXCR4 mAb (A-145). β-actin serves as a control. B) The degradation rate of HA-tagged CXCR4 in empty vector- or CD63ΔN-transduced MAGIC-5 cells. The degradation of CXCR4 in the presence of CHX was assessed by Western blotting. The decay graph shows average of three independent trials (right panel). The images of one representative blot are also shown. Tubulin serves as a control. C) Intracellular CXCR4 was found in CD63ΔN-transduced MAGIC-5 cells. Cells were stained with an anti-CXCR4 mAb (A-145), and analyzed by confocal microscopy. Images were acquired through BPF 500–520 nm (CXCR4: green) and BPF 420–470 nm (Hoechst: blue). Scale bars, 10 μm. D, E) Intracellular CXCR4 was detected in the presence of CD63ΔN. Empty vector- or CD63ΔN-transduced MAGIC-5 cells transfected with phrGFPCXCR4 (D), and 293T cells co-transfected with phrGFPCXCR4 and empty vector or CD63ΔN DNA (E), were analyzed by confocal microscopy. Images were acquired through band-pass filters (BPF) 500–520 nm (GFP: green) and BPF 420–470 nm (Hoechst: blue). Scale bars, 10 μm. DIC images are also shown (lower panel).

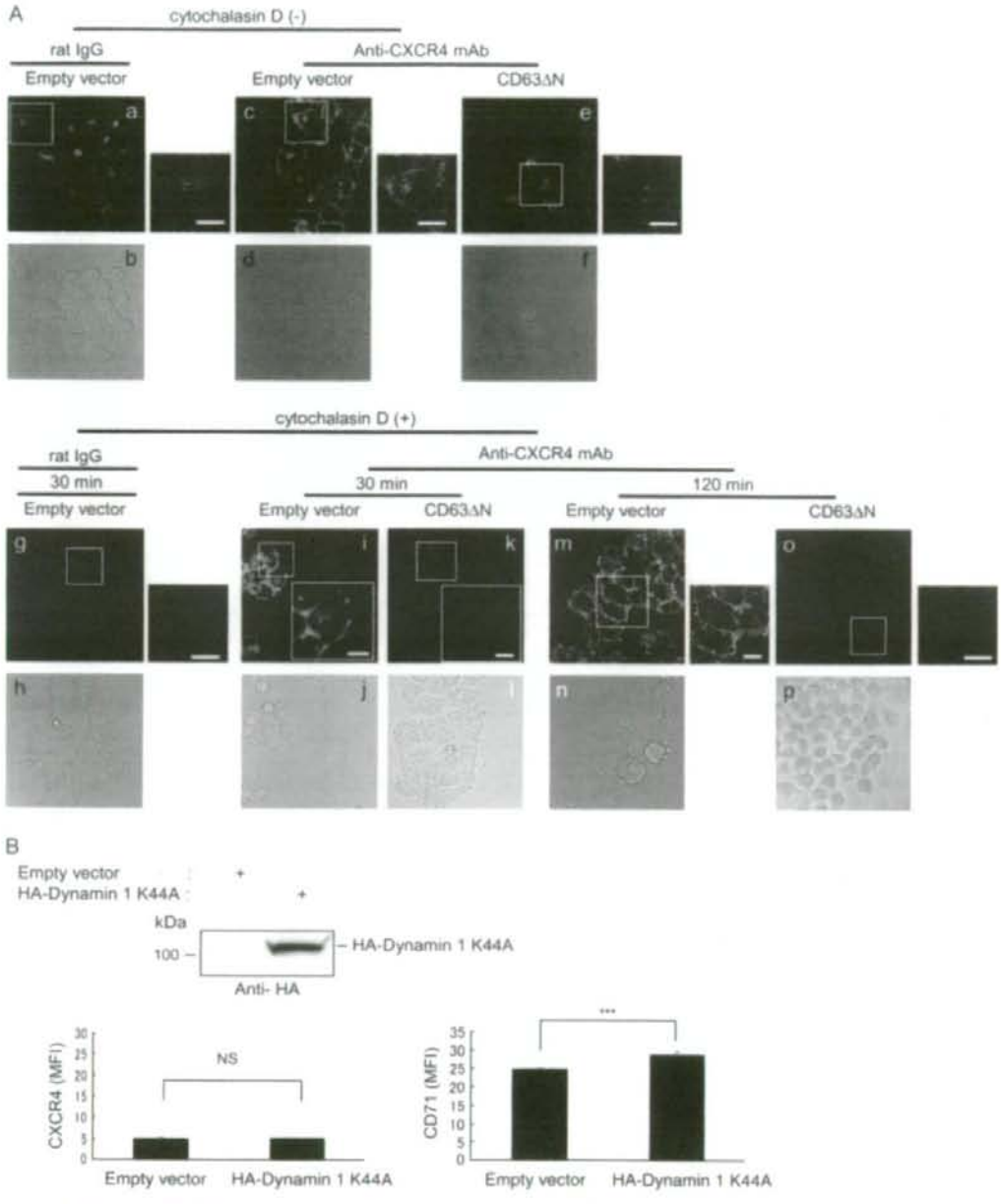

Figure 5: Absence of CXCR4 from cell surface might not be because of dynamin-dependent internalization. A) No detectable CXCR4 surface expression on CD63ΔN-transduced MAGIC-5 cells. Empty vector- and CD63ΔN-transduced cells were cultured in the presence of an FITC-labeled anti-CXCR4 mAb (A-145) for 30 min (a–f) and then analyzed by confocal microscopy. Cells supplemented with cytochalasin D (5 μM) were also cultured for 30 min (g–l) or 120 min (m–p). Enlarged images are shown in white boxes. Images were acquired through BPF 500–520 nm (CXCR4: green). Scale bars, 10 μm. DIC images are also shown (lower panel). B) CD71 but not CXCR4 surface expression was increased by dominant negative mutant of dynamin 1-transfection. CD63ΔN-transduced MAGIC-5 cells were transfected with HA-tagged Dynamin 1 K44A DNA. The expression of HA-tagged protein was confirmed by Western blotting (upper panel), and CXCR4 (lower left panel) or CD71 (lower right panel) surface expression was measured by flow cytometry. MFI of CXCR4 or CD71 was shown. Data are represented as mean ± SED, $n = 4$, $^{***}P < 0.05$, NS, not significant.

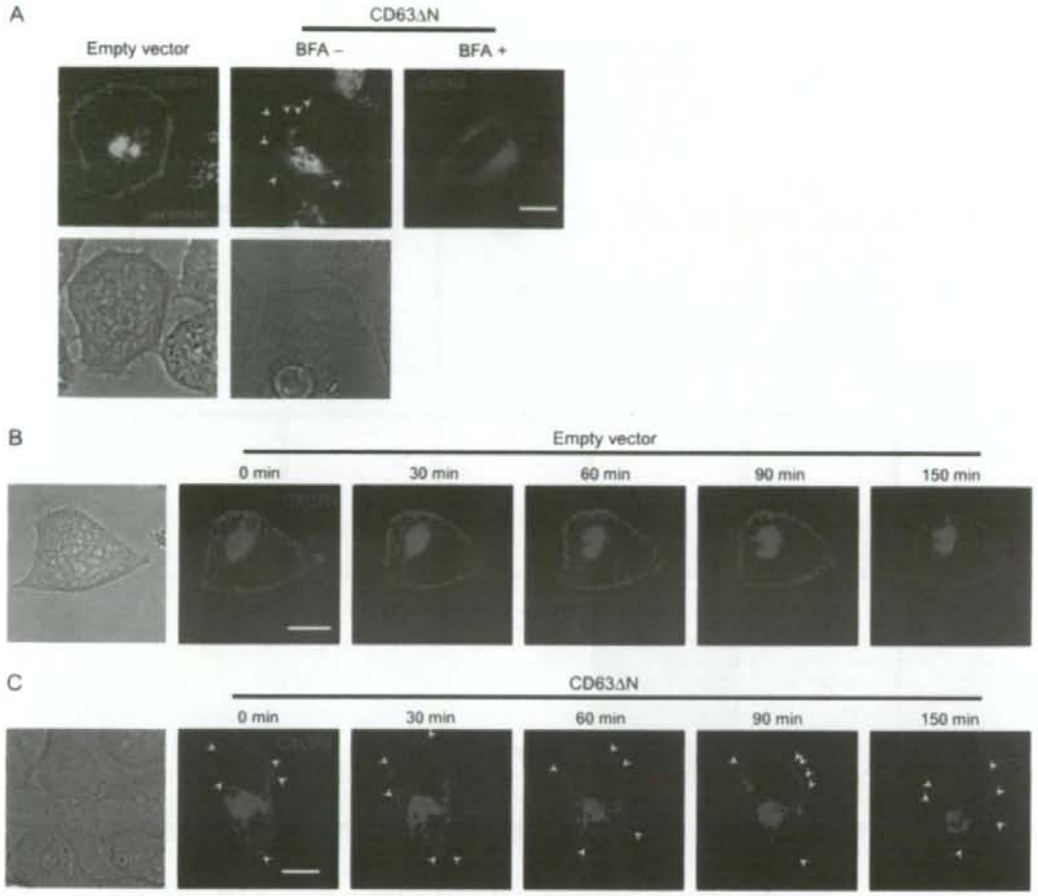

Figure 6: Intracellular trafficking of CXCR4 via transport vesicles is not inhibited. A) Localization of CXCR4 in live cells. MAGIC-5 cells were transfected with pHalo-CXCR4, stained with the Halo-ligand and ceramide (Golgi apparatus) and analyzed by confocal microscopy. Right panel shows cells cultured in medium containing 50 μg/mL of BFA without ceramide-staining. Images were acquired through band-pass filters (BPF) 500–520 nm (ceramide: green) and BPF 570–610 nm (CXCR4: magenta). Arrow heads indicate CXCR4-containing vesicles. Scale bars, 10 μm. DIC images are also shown (lower panel). B, C) Longitudinal analyses on the distribution of CXCR4. Cells were followed with confocal microscopy at the indicated time after initiation of the trace. Empty vector-transduced (B) and CD63ΔN-transduced (C) MAGIC-5 cells were studied. Arrow heads in (C) indicate CXCR4-containing vesicles in CD63ΔN-transduced cells. Scale bars, 10 μm. DIC images are also shown (first panels in B, C). D, E) empty vector-transduced (D) or CD63ΔN- transduced (E) MAGIC-5 cells were transfected with CXCR4EGFP and analyzed using TIRFM. DIC images are shown (upper right panels in D and E). Enlarged images from upper left panels in D and E (box) taken at 1-second interval are shown in middle and lower panels. Fusion-like processes between the vesicle and the plasma membrane was detected in empty vector-transduced but not in CD63ΔN-transduced cells. Arrows in middle panels in (E) indicate fusion-like process between a vesicle and the plasma membrane. Images were acquired through BPF 509–547 nm (GFP). Dotted lines indicate the plasma membrane. Scale bars, 10 μm (upper panel) and 1.7 μm (lower panel). sec, second. Figure 6 continued on next page.

number of the vesicles in both empty vector- and CD63ΔN-transduced cells (Table 1). These data suggest that the CD63ΔN-induced CXCR4 mislocalization is not because of inhibition of CXCR4 trafficking via transport vesicles. CXCR4 is suggested to be transported to intracellular organelles, but not to the plasma membrane. As precise quantification of fusion to the plasma membrane was difficult in this assay, we were not able to quantify the fusion events. Interestingly, however, we could capture some fusion-like processes between CXCR4-containing vesicles and the plasma membrane in empty vector-transduced cells (one of them was shown in Figure 6D, arrows in middle panels) but not in CD63ΔN-transduced cells (Figure 6E).

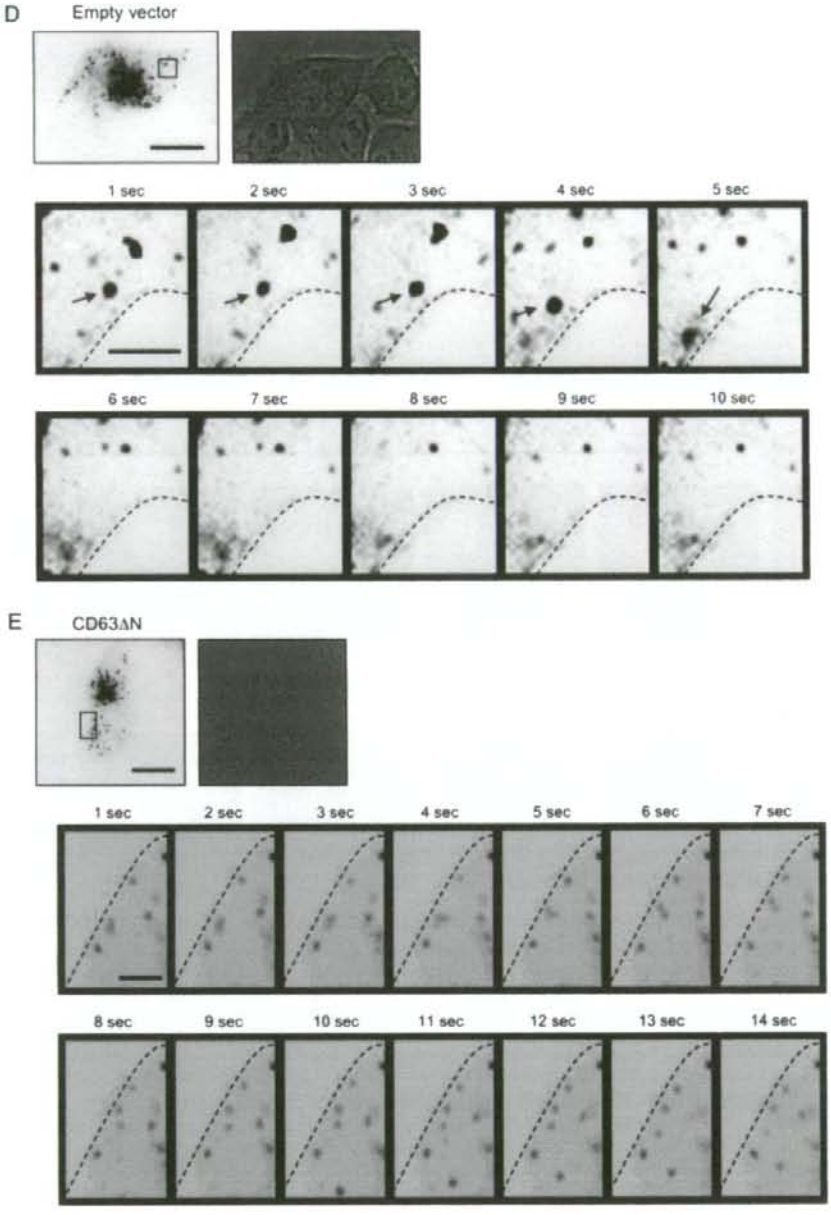

Figure 6: Continued from previous page.

Mislocalized CXCR4 appears to be destined in the late endosomes/lysosomes

To investigate the mislocalization of CXCR4 further, we carried out a series of immunofluorescent staining using antibodies against marker molecules in several different organelles. Figure 7A shows that the intracellular CXCR4 in CD63ΔN-transduced cells were predominantly located in the *cis*-Golgi (Golgi matrix protein of 130 kDa: GM130), the TGN (p230) and the late endosomes/lysosomes (LAMP-1), but not in the early endosomes (early endosome antigen 1,

Table 1: Quantification of CXCR4-containing vesicles[a]

	Counted cells	Total	Average (per a cell[b])
Empty vector	9	1144	127.1
CD63ΔN	19	2257	118.8

[a]Number of vesicles was counted by Basic Metamorph software.
[b]Number of vesicles was divided by numbers of cells.

EEA1). It was also partly located in the ER (calnexin) and the vesicles and tubular clusters (ERGIC-53). We also found that a large fraction of intracellular CXCR4 co-localized with lysosome marker, a low internal pH indicator; LysoTracker in CD63ΔN-transduced MAGIC-5 cells transfected with phrGFPCXCR4 (Figure 7A, right panels). The ratio of the merged area where CXCR4 localized with each intracellular organelle is shown in Figure 7B. This graph shows that no CXCR4 is retained in any specific organelle and that the CXCR4 appears to be transported to the late endosomes/lysosomes. By contrast, in empty vector-transduced cells, CXCR4 was mainly found at the plasma membrane and additionally in the ER (Figure S2). We next assessed whether or not CXCR4 is destined to the lysosome-dependent degradation in CD63ΔN-transduced cells using lysosomal inhibitors (chloroquine, CHQ or concanamycin A, CMA) (Figure 7C). In the inhibitor-treated cells, CXCR4 degradation after CHX treatment was clearly inhibited, indicating that most CXCR4 was transported to lysosomes and subsequently degraded in CD63ΔN-transduced cells.

CD63ΔN co-localizes and interacts with CXCR4

To investigate the intracellular co-localization of CD63ΔN and CXCR4, we prepared a FLAG-tagged CD63ΔN (FLAGCD63ΔN)-expressing lentiviral vector and confirmed that its ability to suppress CXCR4 surface expression was similar to that of untagged vector (data not shown). Then, we examined the co-localization of CD63ΔN and CXCR4 in FLAGCD63ΔN-transduced MAGIC-5 cells using confocal microscopy. As shown in Figure 8A, CD63ΔN molecules mainly overlapped with CXCR4 in the perinuclear region. Similar co-localization of CD63ΔN and CXCR4 was also reproduced in 293T cells co-transfected with phrGFPCXCR4 and a red fluorescent protein–tagged CD63ΔN DNA (DsRed-CD63ΔN) (data not shown). Further immunofluorescent staining experiments using antibodies against organelles marker molecules indicated that CD63ΔN was mainly localized in the late endosomes and the TGN (Figure 8B). To gain insight into the relationship between CD63ΔN and CXCR4, we next examined intracellular interaction between these molecules. In addition to CD63ΔN, CD63wt was also examined. As shown in right panel of Figure 8C, CD63ΔN and CD63wt co-precipitated with CXCR4 in 293T cells co-transfected with hemagglutinin (HA)-tagged CXCR4 DNA (pHA-CXCR4) and a FLAG-tagged CD63ΔN or CD63wt DNA. The affinity of CD63ΔN to CXCR4 appeared to be higher than that of CD63wt. CD63wt but not CD63ΔN had an ability to interact with MT1-MMP as reported previously (20).

Requirement of a CXCR4 C-terminal cytoplasmic tail for CD63ΔN-induced suppression in CXCR4 surface expression

To explore the responsible region of CXCR4 for the CD63ΔN-induced suppression, we used a series of EGFP-tagged CXCR4 C-terminal cytoplasmic tail-deletion mutant DNA (C-terminal tail; 14 amino acids from C-termini) (26) (Figure 9A) and transfected them into empty vector- or CD63ΔN-transduced MAGIC-5 cells. Having confirmed that these mutants were expressed on the cell surface of empty vector-transduced cells (data not shown), we measured CXCR4 mutant surface expression on CD63ΔN-transduced cells using flow cytometry. Interestingly, we found that CXCR4 surface expression was sustained in cells transfected with a mutant lacking six amino acids in the C-terminal tail (Figure 9B). The distribution of CXCR4EGFP or these mutants in CD63ΔN-transduced MAGIC-5 cells is also shown in Figure 9C. These mutants but not CXCR4EGFP (wild type) were localized at the plasma membrane. From these data, we deduced that this six amino acid-deletion provided resistance to the CD63ΔN-induced suppression of CXCR4 surface expression. We observed a similar phenomenon in 293T cells co-transfected with CD63ΔN and EGFP-tagged CXCR4-deletion mutant DNA (data not shown). These results indicate that the C-terminal six amino acids (^{347}SSFHSS^{352}) are involved in the CD63ΔN-induced suppression of CXCR4.

Discussion

In this study, we successfully identified a mutant of a tetraspanin protein (CD63ΔN) as an inhibitor of X4 HIV-1-induced CPE by our screening strategy using a novel cDNA library-expressing lentiviral vector system (2). Then, we showed that CD63ΔN inhibited X4 HIV-1 infection (Figure 1E,G). The inhibition was observed in X4 HIV-1 but not in MLV-pseudotyped HIV-1 (Figure 1F) or R5 HIV-1 (Figure 1G). Because the difference between X4 HIV-1 and R5 HIV-1 lies upon co-receptor usage at the viral entry, we predicted and confirmed that CD63ΔN induced the suppression of CXCR4 surface expression (Figure 2A,D). These data provide the evidence that localization of co-receptor molecules at the plasma membrane is crucial for HIV-1 entry and by depleting the surface expression of co-receptor proteins, HIV-1 target cells can effectively escape from its infection.

It has been shown that anti-CD63 Ab (27) or recombinant soluble CD63-EC2 proteins (28) inhibited HIV infection in macrophages without affecting expression of CD4 or co-receptor. However, we clearly showed that a CD63 N-terminal deletion mutant blocks X4 HIV-1 entry via specific suppression of CXCR4 surface expression on target cells (Figure 2A,D,E–G). It has not been yet reported that CD63 or its mutants induce downregulation of CXCR4.

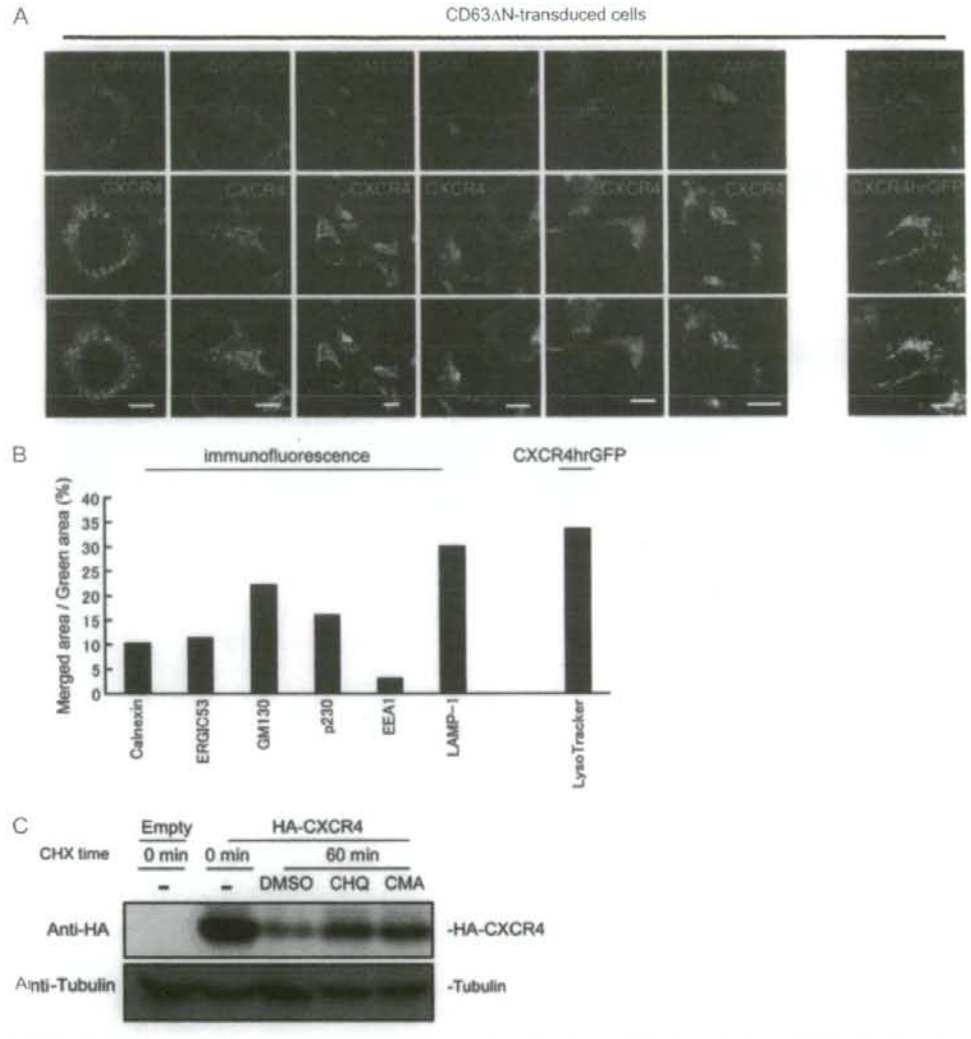

Figure 7: CXCR4 was transported only toward intracellular organelles. A) Co-localization of CXCR4 with intracellular organelles in CD63ΔN-transduced MAGIC-5 cells. Images were acquired through band-pass filters (BPF) 500–520 nm (CXCR4 and CXCR4hrGFP: green), BPF 650–700 nm (intracellular organelles: magenta) and BPF 420–450 nm (LysoTracker: magenta). Merged images are shown in bottom. Scale bars, 10 μm. Calnexin: ER; ERGIC53: Vesicular-tubular transport complex (VTCs); GM130: *cis*-Golgi; p230: TGN; EEA1: early endosomes; and LAMP-1: late endosomes. B) The ratio of merged area where CXCR4 co-localized with each intracellular organelle in (A) (merged area/CXCR4 area) was shown. C) The lysosome-dependent degradation of HA-tagged CXCR4 in CD63ΔN-transduced MAGIC-5 cells. The degradation of CXCR4 in the presence of CHX with two classes of lysosomal inhibitors, CHQ (50 μg/mL), CMA (20 μg/mL) or vehicle (DMSO), was assessed by Western blotting. Tubulin served as a control. The results of one of three, independently conducted, experiments are shown.

Although these previous findings and our presented phenomena seem to occur by distinct mechanisms, it might be true that CD63 has some functions in HIV infection.

By flow cytometric analyses, we confirmed the CD63ΔN-induced CXCR4 downregulation in MT-4 (Figure 2A), MAGIC-5 (Figure 2D) and 293T cells (data not shown) as well as human primary $CD4^+$ T cells (Figure 2F), natural target cells for HIV-1. These data suggest that this CD63ΔN-induced suppression is not a cell type-dependent phenomenon. The significant but lower suppression of CXCR4 in $CD4^+$ T cells (Figure 2F) can be explained by the lower efficiency of lentiviral transduction. Also, primary $CD4^+$ T cells needed to be activated with immobilized

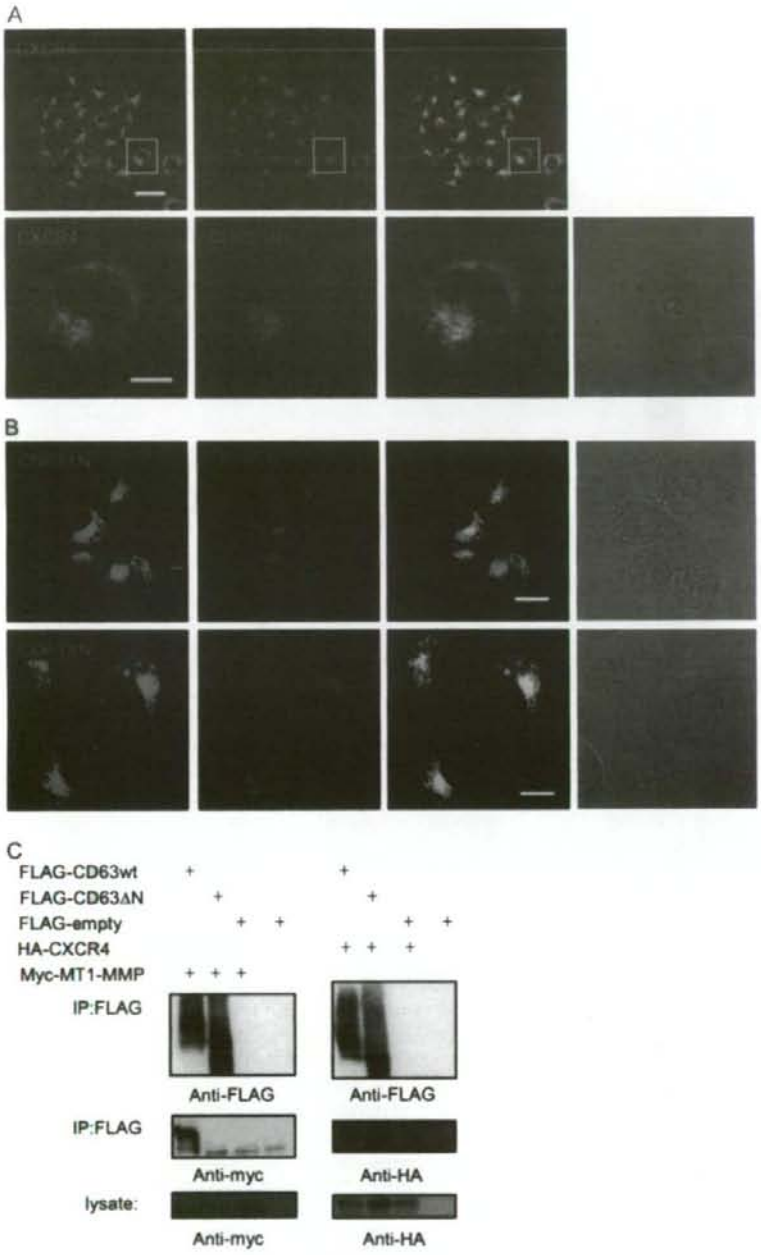

Figure 8: Co-distribution and interaction of CD63ΔN with CXCR4. A) Localization of CXCR4 and CD63ΔN. FLAGCD63ΔN-transduced MAGIC-5 cells were stained with an anti-CXCR4 mAb and an anti-FLAG pAb. Images were acquired through band-pass filters (BPF) 500–520 nm (CXCR4: green) and BPF 650–700 nm (FLAG: magenta) and merged images are shown. Scale bars, 50 μm (upper panels) and 10 μm (lower panels). B) Co-localization of FLAGCD63ΔN with intracellular organelles in FLAGCD63ΔN-transduced MAGIC-5 cells. Images were acquired through BPF 500–520 nm (FLAG: green) and BPF 650–700 nm (intracellular organelles: magenta). Merged images are shown in third panels. Scale bars, 10 μm. LAMP-1, late endosomes; and p230: TGN. C) Molecular interaction between CXCR4 and CD63ΔN or CD63wt. FLAG-tagged CD63ΔN or CD63wt were immunoprecipitated (IP) with an anti-FLAG mAbs and immunoblotted with an anti-HA and an anti-FLAG mAb (right panel). Lysate were also subjected to Western blot to detect expression of HA-tagged CXCR4. Interaction between CD63wt and MT1-MMP was shown as a control (left panel). The results of one of three, independently conducted, experiments are shown.

anti-CD3/CD28 mAbs during lentiviral transduction. As CXCR4 surface expression is reduced on activated $CD4^+$ T cells (29), primary $CD4^+$ T cells had lower expression of CXCR4 compared with that of cell lines to start with. In addition to flow cytometric analyses, we confirmed the CXCR4 downregulation by immunofluorescent analysis without permeabilization (Figure 2E) and the reduced response to SDF-1 by CD63ΔN-transduced cells (Figure 2G).

CD63 is known to form TEMs on the plasma membrane with other tetraspanin proteins (11). Do TEMs play any role

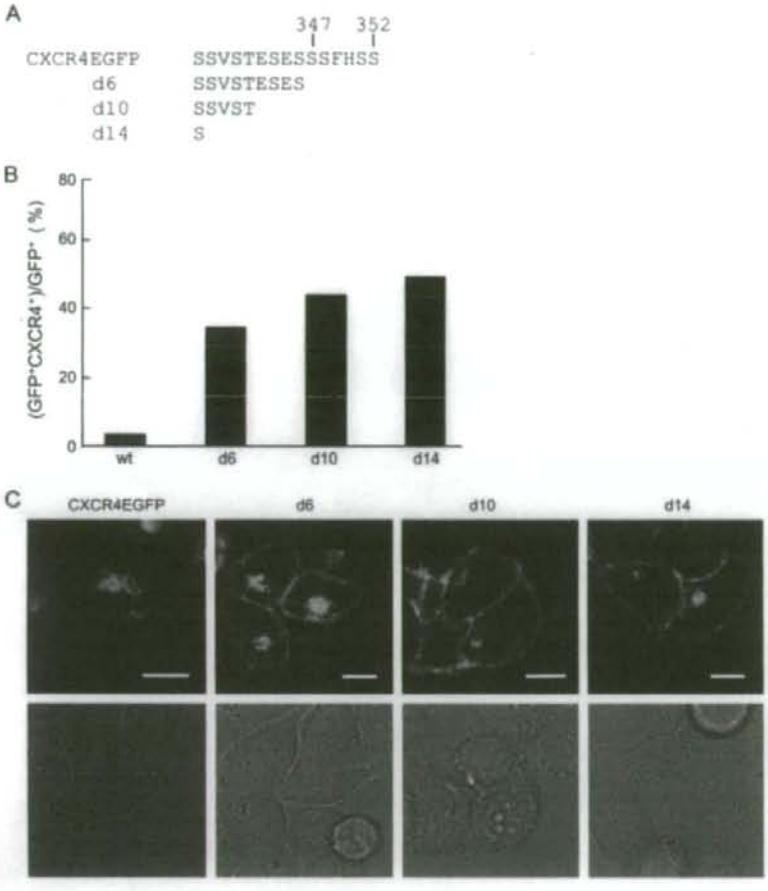

Figure 9: Requirement of CXCR4 C-terminal cytoplasmic tail for CD63ΔN-induced suppression in CXCR4 surface expression. A) Amino acid sequence of the C-terminal tail of CXCR4. Shown is the amino acid sequence (single-letter code) of the C-terminal tail of wild-type CXCR4, along with the various mutants used in this experiment. B) Sustainment of CXCR4 surface expression from its C-terminal tail-deletion mutant in CD63ΔN-transduced cells. CD63ΔN-transduced MAGIC-5 cells were transfected with CXCR4EGFP, or its C-terminal tail-deletion mutants (d6, d10 or d14), and CXCR4 surface expression and GFP were measured by flow cytometry. Percentage of GFP^+CXCR4^+ cells out of total GFP^+ cells is shown. Results of one of three, independently conducted, experiments are shown. C) Expression at the plasma membrane was detected for d6, d10 or d14 mutants but not for CXCR4EGFP in the presence of CD63ΔN. CD63ΔN-transduced MAGIC-5 cells transfected with CXCR4EGFP or the mutant DNA, were analyzed by confocal microscopy. Images were acquired through band-pass filters 500–520 nm (GFP: green). Scale bars, 10 μm. DIC images are also shown (lower panel).

in the CD63ΔN-induced suppression? The first question was whether CD63ΔN has any effect on the surface expression of other tetraspanin proteins. The cell surface expression of other tetraspanin proteins such as CD9, CD53, CD81, CD82 and CD151 was not changed in CD63ΔN-transduced MAGIC-5 cells (data not shown) as well as that of CD4, CCR5 and CD71 (Figure 2D). This result suggests that the CD63ΔN-induced suppression might not be caused by any changes of TEMs. The second question was whether other tetraspanin proteins inhibit CXCR4 surface expression. Although CD63wt suppressed CXCR4 surface expression (Figure 2A), we found that CD9, CD81 or CD151 have no suppressive activity on CXCR4 surface expression in MT-4 cells (data not shown). These data strongly suggested that TEMs are not involved in the CD63ΔN-induced suppression. Furthermore, we also found that knockdown of endogenous CD63 resulted in increase of CXCR4 surface expression (Figure 3C). Thus, we deduced that CD63 itself possesses some suppressive ability for CXCR4 surface expression, probably in a TEMs-independent manner.

We next showed that the CD63ΔN-induced disappearance of surface CXCR4 is not because of suppression on gene expression (Figure 4A) or rapid degradation (Figure 4B), but most likely the result of mislocalization of CXCR4. From immunofluorescent analysis and confocal microscopic analysis using phrGFPCXCR4, we found large amounts of intracellular CXCR4 in CD63ΔN-transduced cells but not at the plasma membrane (Figure 4C–E). There have been many reports on the downregulation of cell surface proteins caused by mislocalization. The downregulation of major histocompatibility complex (MHC) class I molecules from the cell surface upon viral infection may be the most well known (30). To evade the monitoring of cytotoxic T lymphocyte, some viral proteins induce mislocalization of MHC class I molecules by many strategies such as (i) rapid internalization, (ii) inhibition of egress from the ER and (iii) re-routing of MHC class I molecules. MHC class I molecules such as human leukocyte antigen (HLA)-A and -B are endocytosed by the HIV Nef and phosphofurin acidic cluster sorting protein-1 in the ARF 6 pathway (31,32). MHC class I molecules (HLA) are prevented from

being transported to the plasma membrane by the adenovirus gene product E3/19K (E19) (33). The re-routing of MHC class I molecules to the lysosome is induced by the human herpesvirus 7 glycoprotein U21 and the mouse cytomegalovirus early gene product (gp48) (34,35).

In the case of CXCR4, rapid internalization was our first guess because CD63 has been reported to play roles in endocytosis of interaction partners such as the HKβ (19) and MT1-MMP (20). Duffield et al. showed that the HKβ interacted with CD63 and the HKβ/CD63 complex was efficiently internalized. When the interaction between CD63 and AP complexes was disrupted, HKβ was not able to be internalized from the cell surface and was retained at the plasma membrane. Takino et al. showed that CD63 formed a complex with MT1-MMP and was involved in internalization, lysosomal targeting and proteolysis of MT1-MMP via LSM-dependent endocytosis (20). These reports suggest that CD63 acts as a mediator between the interaction partners and AP-2 complexes to enhance internalization of the CD63/interaction partner complex (36). In CD63ΔN-transduced cells, however, we could not detect any CXCR4 surface expression for 120 min in anti-CXCR4 mAb feeding experiments under conditions that inhibit actin polymerization (Figure 5A) and found that CD63ΔN-induced suppression of surface CXCR4 expression was not able to be rescued by the dominant negative mutant of dynamin 1 (Figure 5B). Moreover, we found that the CD63ΔN-induced inhibition of X4 HIV infection and suppression of CXCR4 surface expression were not impaired dramatically by LSM deletion (Figures 1E and 2A) and a CD63 mutant lacking LSM (CD63ΔL) still maintained suppressive activity (data not shown). Thus, these data suggest that this CXCR4 down-regulation might not be the result of dynamin-dependent or AP complex-dependent endocytosis. Furthermore, we found that in CD63ΔN-transduced cells, little intracellular CXCR4 was found in the early endosomes (Figure 7A, EEA1). As endocytosed membrane proteins are first collected in the early endosome, this data support the hypothesis that there is little CXCR4 endocytosis in CD63ΔN-transduced cells. Although role of CD63 in these previous studies and that of CD63ΔN in our study appears to be distinct, CD63 has some roles in intracellular trafficking of other proteins.

We showed that intracellular trafficking of CXCR4 via vesicular transport was not stopped by CD63ΔN transduction. The number of CXCR4-containing transport vesicles was not reduced by CD63ΔN transduction (Table 1). We showed that there is no ER retention of CXCR4 in CD63ΔN-transduced cells because the distribution of CXCR4 in CD63ΔN-transduced cells was distinct from that in cells with BFA-induced CXCR4 retention in the ER (Figure 6A). Furthermore, CXCR4 seemed to be distributed in the Golgi of CD63ΔN-transduced cells (Figure 7A,B). This is direct evidence that further rejects the hypothesis that CXCR4 is retained in ER. The fact that a large amount of CXCR4 was also found in the late endosomes/lysosome (Figure 7A,B) indicates the existence of post-Golgi transportation and brings up the possibility that transportation of CXCR4 takes place in CD63ΔN-transduced cells. If lysosome-dependent degradation of CXCR4 indeed takes place in these cells, it should be able to be inhibited by lysosomal inhibitors (CHQ or CMA) treatment. When CD63ΔN-transduced cells were treated with CHX and CHQ or CMA, the degradation of CXCR4 was greatly inhibited (Figure 7C). This biochemical assay confirms the lysosome-dependent degradation of CXCR4, and together with the immunofluorescent analysis, shows that CXCR4 is localized and destroyed in the lysosome.

In this study, we found that six amino acids (^{347}SSFHSS^{352}) in the CXCR4 C-terminal tail were crucial for the CD63ΔN-induced CXCR4 mislocalization (Figure 9B, C). Some motifs in the CXCR4 C-terminal region such as di-leucine motif (^{328}IL^{329}) (37) and the integrity of specific serine residues in the C-terminal tail (S^{324}, S^{325}, S^{338} and S^{339}) (7) have been found to be important for localization of CXCR4. However, all the currently known motifs are involved in the internalization of CXCR4.

We also showed that CD63ΔN co-localized with CXCR4 (Figure 8A) and interacted with CXCR4 (Figure 8C). To investigate the importance of this interaction, we assessed whether the resistant mutant in Figure 9 (d6) can associate with CD63ΔN. Deletion of the six amino acids failed to abrogate association with CD63ΔN (data not shown), indicating that these amino acids are not the binding motif for CD63 (CD63ΔN). However, interaction between CXCR4 and CD63ΔN may still be a part of mechanism of changes in CXCR4 trafficking. There may be subtle differences in affinities of wild-type CXCR4 and d6 mutant to CD63ΔN, or CD63ΔN may take CXCR4 to another interacting protein, which binds through the C-terminal amino acids. In fact, direct molecular interaction is not necessary in the case of trafficking regulation of CD19 by another tetraspanin, CD81 (38). CD81 has been reported to have roles in transportation of CD19 to the plasma membrane (36,39,40). Moreover, a series of subsequent studies using many CD81 mutants showed that CD81 plays a variety of roles using different CD81 domains in different cellular compartments (38). CD63 might also have variety of roles in intracellular trafficking. In fact, a large amount of CD63ΔN is in the Golgi (Figure 8B), where more than 35% of total CXCR4 in CD63ΔN-transduced cells was also found (Figures 6C and 7A,B). Since it remains unknown how CXCR4 is sorted in the Golgi, further study is required to understand the mechanism that directs of CXCR4 trafficking at the Golgi apparatus.

In summary, we successfully identified a new X4 HIV-1 entry inhibitor, CD63ΔN. CD63ΔN induced suppression of CXCR4 surface expression, and this phenomenon appears to be caused by mislocalization of CXCR4. Intracellular CXCR4 was distributed not at the plasma membrane but

in intracellular organelles such as the Golgi and the late endosomes/lysosomes and it was degraded in the lysosome. In addition, from CD63-overexpression or depletion experiments, CD63 itself appears to have a role in influencing the level of CXCR4 surface expression, which may be one of its physiological functions.

Materials and Methods

Cells and transfection

Human 293T and MAGIC-5 cells (41) and MT-4 cells were maintained as previously described (2). PBMC were prepared from a HIV-1-seronegative donor, and $CD4^+$ cells were isolated using a CD4-positive isolation kit (Dynal Biotech). These cells were stimulated with CD3/CD28 T-cell expander (Dynal) and maintained in RPMI-1640 containing 10% fetal calf serum and 100 U/mL of IL-2. For transfection, Lipofectamin 2000 transfection reagent (Invitrogen), TransIT LT-1 transfection reagent (Takara) or the calcium phosphate method were used. BFA, CMA, CHX and dimethyl sulfoxide (DMSO) were purchased from Sigma and CHQ was purchased from Wako.

DNA construction

Lentiviral vector DNA, CSII-CDF-GATEWAY-IRES-$H2K^k$, was constructed through the replacement of *hrGFP* with *H-2K*^{k} (Daiichi Pure Chemicals) in pYK005C (2). *cd63* and *cd63ΔN* was cloned from the human PBL cDNA library into a CMV promoter-driven expression plasmid, pCMV-SPORT6 (Invitrogen). Human *cxcr4* was cloned into pCMV-SPORT6 or an upstream site of *hrgfp* tag in pIRES-hrGFP (Stratagene) (pCXCR4 and phrGFPCXCR4) and pCXCR4 FL GFP, d-6 GFP, d-10 GFP, d-14 GFP (26) were used. *cd63wt*, *cd63ΔN* and *cd63ΔNL*, were cloned into p3XFLAG-CMV-10 (Sigma) and FLAG-tagged *cd63ΔN* was transferred in pCMV-SPORT6. *cxcr4* was cloned into an upstream site of a *halo* tag and downstream of HA tag in pCMV-SPORT6, respectively (pHalo-CXCR4 and pHA-CXCR4). A cDNA on pCMV-SPORT6 was transferred into CSII-CDF-GATEWAY-IRES-$H2K^k$ through BP and LR reaction on Gateway cloning system (Invitrogen). An EGFP-expression *env*-deleted HIV-1 plasmid DNA, pNL-EGFPΔenv, was constructed with a flameshift introduced at the *Nhe*I site of the *env* in pNLEGFP by blunting and religation. pcDNA3.1(−) HA-Dyn1 K44A (MBA-93) was obtained from ATCC. The nucleotide sequences of all constructs were confirmed using ABI 377 auto-sequencer.

Antibodies

The following primary unconjugated antibodies against human proteins were used: rat anti-CXCR4 mAbs (A-80, A-145) (42), a mouse anti-CD63 mAb, a goat anti-EEA1 polyclonal antibody (pAb), a mouse anti-LAMP-1 mAb (Santa Cruz Biotechnology), a mouse anti-ERGIC53 mAb (Alexis Biochemicals), a mouse anti-GM130 mAb, a mouse anti-p230 mAb (BD Transduction), a rabbit anti-calnexin pAb (Stressgen Bioreagents), a mouse anti-tubulin mAbs (Sigma) and a mouse anti-β-actin mAb (Cell Signaling Technology). A mouse mAb and a rabbit pAb against FLAG peptides, a mouse mAbs against c-Myc peptides and a horseradish peroxidase (HRP)-conjugated rat mAb against HA peptides were purchased from Sigma, Clontech and Roche, respectively. FITC-conjugated mAbs against CD25 and a phycoerythrin (PE)-conjugated mAb against CCR5 were purchased from BD Pharmingen, FITC or PE-conjugated mouse anti-mouse $H\text{-}2K^k$ mAbs were purchased from Cedarlane and a PE-conjugated mouse mAb against CD4 and FITC-conjugated mAbs against CD71 were purchased from Dako and Immunotech, respectively. Sera from HIV-1-infected people were used for detecting HIV-1 antigens. The following second pAbs were used: an FITC-conjugated goat anti-rat IgG antibody (American Qualex), an Alexa488-conjugated goat anti-mouse IgG pAb (Molecular Probes), Cy5-conjugated donkey pAbs against rabbit IgG, mouse IgG or goat IgG, respectively, a biotin-conjugated donkey anti-rat IgG pAb (Chemicon), a biotin-conjugated goat anti-human IgG pAb (Vector Laboratories) and a HRP-conjugated anti-mouse IgG pAb (Cell Signaling). HRP- (Zymed), PerCP- (BD Bioscience) or Alexa 488- (Molecular Probes)-conjugated streptavidin was also used.

Small interfering RNA

Synthetic siRNAs directed against *cd63* (no. 199: 5′-ACAGCUUGUCCUGAGUCAGACCAUA-3′, no. 317: 5′-GCCUGCAAGGAGAACUAUUGUCUUA-3′ and no. 844: 5′-GAGUGGAAUAGUAUCCUCCAGGUUU-3′) and Stealth RNAi Negative Control Duplexes Medium GC Duplex were purchased from Invitrogen. Transfection was performed using Lipofectamine 2000.

Flow cytometric analysis

Flow cytometric analyses using cell line were performed as previously described (2). In case of T-cells staining, Fc receptor blocker (Dynal) was used. Data was collected using FACScan or FACScalibur (BD Bioscience) and analyzed using WinMDI software.

Immunoprecipitations and Western blotting

CXCR4 was detected as previously described (42). To detect FLAG-tagged protein, cells were scraped in triple detergent containing 1% Igepal (Sigma), 0.1% SDS, 0.5% sodium deoxycholate in 20 mM Tris–HCl (pH 8) – 0.15 M NaCl – protease inhibitor cocktail Complete (Roche). For samples of deglycosylation procedure, immunoprecipitation was required. After supplementation of an anti-FLAG mAb and incubation for 12 h at 4°C in the presence of protein G-sepharose (Amersham Biosciences), immunoprecipitants were treated with Glycoprotein Deglycosylation Kit (Calbiochem) according to the manufacturer's protocol. Interaction between CD63 and CXCR4 was also detected as described above except detergent buffer, instead of triple detergent, single detergent containing 1% Triton X-100 in 50 mM Tris–HCl (pH 8) – 0.15 M NaCl – protease inhibitor cocktail Complete, was used. Immunoprecipitation and immunoblotting of MT1-MMP were carried out as previously described (20). For degradation assay, cells transfected with pHA-CXCR4 were incubated in the presence of 15 μg/mL CHX with either 50 μg/mL CHQ, 20 μg/mL CMA or vehicle control (DMSO) and harvested at the indicated times. Cells were lysed with single detergent.

HIV-1 infection

Lentiviral vector and HIV-1 preparation were carried out as described previously (2). Cells transduced with the original, CD63 mutant fragments (clone 12.03 and clone 12.22) were infected with $HIV\text{-}1_{NL4\text{-}3}$ and expression of HIV-1 antigen was examined 4 dpi using an anti-HIV-1 human serum. CD63wt or CD63 mutant-transduced cells were infected with NL-EGFP (24) at a MOI of 0.1. Three dpi, dual color flow cytometric analysis was performed. To prepare amphotropic MLV Env-pseudotyped HIV-1, 293T cells were co-transfected with pNL4-3Δenv and pJD-1 (43). Forty-eight hours later, culture supernatants were collected and used for infection. CD63ΔN-transduced cells were infected with $HIV\text{-}1_{NL4\text{-}3}$ or $HIV\text{-}1_{JR\text{-}CSF}$ (44) at a MOI of 2 and then the culture supernatant was harvested. The level of HIV-1 $p24^{gag}$ antigen was measured by ELISA (ZeptoMetrix Corp.). To detect HIV-1 DNA by polymerase chain reaction (PCR), cells were harvested 1 dpi and PCR was performed with HIV *Tat/Rev*-specific primers (45). To prepare heat inactivated HIV-1 as a negative control, viruses were incubated at 65°C for 30 min.

Chemotaxis assay

Cell migration was assayed in 24-well cell culture chambers using inserts with 8 μm pore membrane (Falcon). Membranes were pre-coated with fibronectin. Buffer including 100 nM of SDF-1 (Wako) and SYTO 24 (Molecular Probes), and MAGIC-5 cells resuspended in OPTI-MEM reduced-serum medium (Gibco) were applied on lower well and upper wells, respectively. After incubation for 12 h, cells on lower surface of the membrane were visualized by SYTO 24 and counted using a fluorescent microscope in three different fields.

Microscopic analyses

For live cell imaging, cells grown on 12-mm glass-bottomed culture dishes (Iwaki) were transfected with appropriate DNA, at 48 h post-transfection stained with HaloTag™-ligand (Promega), NBD C_5-ceramide (Molecular

Probes), Hoechst33342 (Hoechst) or LysoTracker Blue DND-22 (Molecular Probes) according to manufacturer protocols. To detect surface CXCR4 on live cells, cells were incubated with an anti-CXCR4 mAb (A-145) for 30 min at 4°C. In mAb feeding experiments, cells were cultured in medium containing an FITC-conjugated anti-CXCR4 mAb (A-145) and Hoechst, in the presence or absence of 5 μM of cytochalasin D (Sigma). To detect CXCR4, CD63 or FLAG-tagged proteins, cells grown on APS-coated slide glasses (Matsunami) were fixed in 4% (v/v) paraformaldehyde (PFA) for 60 min at 4°C. After washing with PBS, cells were blocked with PBS containing 10% normal donkey serum, followed by an overnight incubation with primary Abs at 4°C. After extensive washing with PBS, cells were incubated with the secondary Abs for 60 min. In case of dual staining, we routinely incubate cells with no, or only one primary Ab, which were served as control for non-specific binding of secondary Abs. To detect CD63, intracellular CXCR4 with intracellular organelle markers or FLAG-tagged CD63ΔN, cells were treated with PBS containing 0.05% saponin for 10 min at room temperature after fixation to enhance permeability. Cells were analyzed at 37°C (live cells) or room temperature (fixed cells) using a 63×/ 1.4-0.60 HCX PL APO objective on a DMIRE2-TCS SP2 AOBS confocal microscope system (both from Leica) or a PLAPON 60× O TIRFM objective on a IX71 TIRF microscope system (all from Olympus). Images were acquired and analyzed using LCS 2.61 (Leica) or Basic Metamorph (Molecular Devices) and processed using Photoshop CS2 (Adobe).

Statistical analysis

The Mann–Whitney's *U*-test and Student's *t*-test were used to determine statistical significance, and $P < 0.05$ was considered significant.

Acknowledgments

We thank the many colleagues who have contributed ideas and help to this project, in particular Naoko Misawa, Kuniko Hieda and Shunsuke Hatta for technical support, Chuanyi Nie for discussion, Prof. Kouji Matsushima for providing CXCR4 plasmid DNA, Prof. Hiroshi Sato for providing Myc-MT1-MMP plasmid DNA and Prof. Hiroshi Kimura for teaching us to manipulate TIRFM. The authors declare no competing financial interests. This work was supported by grants from the Ministry of Health, Labor, and Welfare and the Ministry of Education, Culture, Sports, Science and Technology of JAPAN. T. Y. is a research fellow of the Japan Society for the Promotion of Science.

Supplementary Materials

Figure S1: Nucleotide sequence of *cd63* cDNA. Nucleotide sequences of the wild-type *cd63* cDNA, and that of the cDNA clones (12.03 and 12.22) isolated at the outset of this study and newly cloned cDNA for preparing lentiviral vector, are indicated. Capital letters indicate the translated region (the CD63wt ORF starts at +95 and the CD63ΔN ORF starts at +341). Dashed lines indicate positions showing identical nucleotide sequence to the human *cd63* cDNA in the NCBI database (accession number of human *cd63* cDNA, NM_001780).

Figure S2: Subcellular distribution of CXCR4 in empty vector-transduced cells. Co-localization of CXCR4 with intracellular organelles (calnexin; ER, GM130; *cis*-Golgi, LAMP-1; late endosome) was shown in empty vector-transduced MAGIC-5 cells. Images were acquired through band-pass filters (BPF) 500–520 nm (CXCR4: green) and BPF 650–700 nm (intracellular organelles: magenta). Scale bars, 10 μm. Merged images are shown in bottom.

Supplementary experimental procedures: Microscopic analyses.

Supplemental materials are available as part of the online article at http://www.blackwell-synergy.com

References

1. Goff SP. Retrovirus restriction factors. Mol Cell 2004;16:849–859.
2. Kawano Y, Yoshida T, Hieda K, Aoki J, Miyoshi H, Koyanagi Y. A lentiviral cDNA library employing lambda recombination used to clone an inhibitor of human immunodeficiency virus type 1-induced cell death. J Virol 2004;78:11352–11359.
3. Feng Y, Broder CC, Kennedy PE, Berger EA. HIV-1 entry cofactor: functional cDNA cloning of a seven-transmembrane, G protein-coupled receptor. Science 1996;272:872–877.
4. Oberlin E, Amara A, Bachelerie F, Bessia C, Virelizier JL, Arenzana-Seisdedos F, Schwartz O, Heard JM, Clark-Lewis I, Legler DF, Loetscher M, Baggiolini M, Moser B. The CXC chemokine SDF-1 is the ligand for LESTR/fusin and prevents infection by T-cell-line-adapted HIV-1. Nature 1996;382:833–835.
5. Signoret N, Oldridge J, Pelchen-Matthews A, Klasse PJ, Tran T, Brass LF, Rosenkilde MM, Schwartz TW, Holmes W, Dallas W, Luther MA, Wells TN, Hoxie JA, Marsh M. Phorbol esters and SDF-1 induce rapid endocytosis and down modulation of the chemokine receptor CXCR4. J Cell Biol 1997;139:651–664.
6. Cheng ZJ, Zhao J, Sun Y, Hu W, Wu YL, Cen B, Wu GX, Pei G. Beta-arrestin differentially regulates the chemokine receptor CXCR4-mediated signaling and receptor internalization, and this implicates multiple interaction sites between beta-arrestin and CXCR4. J Biol Chem 2000;275:2479–2485.
7. Orsini MJ, Parent JL, Mundell SJ, Benovic JL, Marchese A. Trafficking of the HIV coreceptor CXCR4. Role of arrestins and identification of residues in the c-terminal tail that mediate receptor internalization. J Biol Chem 1999;274:31076–31086.
8. Marchese A, Benovic JL. Agonist-promoted ubiquitination of the G protein-coupled receptor CXCR4 mediates lysosomal sorting. J Biol Chem 2001;276:45509–45512.
9. Marchese A, Raiborg C, Santini F, Keen JH, Stenmark H, Benovic JL. The E3 ubiquitin ligase AIP4 mediates ubiquitination and sorting of the G protein-coupled receptor CXCR4. Dev Cell 2003;5:709–722.
10. Neel NF, Schutyser E, Sai J, Fan GH, Richmond A. Chemokine receptor internalization and intracellular trafficking. Cytokine Growth Factor Rev 2005;16:637–658.
11. Tarrant JM, Robb L, van Spriel AB, Wright MD. Tetraspanins: molecular organisers of the leukocyte surface. Trends Immunol 2003;24:610–617.
12. Escola JM, Kleijmeer MJ, Stoorvogel W, Griffith JM, Yoshie O, Geuze HJ. Selective enrichment of tetraspan proteins on the internal vesicles of multivesicular endosomes and on exosomes secreted by human B-lymphocytes. J Biol Chem 1998;273:20121–20127.
13. Kobayashi T, Vischer UM, Rosnoblet C, Lebrand C, Lindsay M, Parton RG, Kruithof EK, Gruenberg J. The tetraspanin CD63/lamp3 cycles between endocytic and secretory compartments in human endothelial cells. Mol Biol Cell 2000;11:1829–1843.
14. Metzelaar MJ, Wijngaard PL, Peters PJ, Sixma JJ, Nieuwenhuis HK, Clevers HC. CD63 antigen. A novel lysosomal membrane glycoprotein, cloned by a screening procedure for intracellular antigens in eukaryotic cells. J Biol Chem 1991;266:3239–3245.
15. Rous BA, Reaves BJ, Ihrke G, Briggs JA, Gray SR, Stephens DJ, Banting G, Luzio JP. Role of adaptor complex AP-3 in targeting wild-type and mutated CD63 to lysosomes. Mol Biol Cell 2002;13:1071–1082.
16. Berditchevski F, Tolias KF, Wong K, Carpenter CL, Hemler ME. A novel link between integrins, transmembrane-4 superfamily proteins (CD63 and CD81), and phosphatidylinositol 4-kinase. J Biol Chem 1997;272:2595–2598.
17. Jung KK, Liu XW, Chirco R, Fridman R, Kim HR. Identification of CD63 as a tissue inhibitor of metalloproteinase-1 interacting cell surface protein. EMBO J 2006;25:3934–3942.